Insights into the mechanisms of L. salivarius CECT5713 resistance to freeze-dried storage

Maria Guerrero Sanchez, Stephanie Passot, Sarrah Ghorbal, Sonia Campoy, Monica Olivares, Fernanda Fonseca

Insights into the mechanisms of *L. salivarius* CECT5713 resistance to freeze-dried storage

Maria Guerrero Sanchez[1], Stéphanie Passot[2], Sarrah Ghorbal[2], Sonia Campoy[1], Monica Olivares[1], Fernanda Fonseca[2*]

[1] Biosearch S.A.U (a Kerry® company), R&D Department, 18004 Granada, Spain

[2] Université Paris-Saclay, INRAE, AgroParisTech, UMR SayFood, F-91120 Palaiseau, France

*Correspondance mail: fernanda.fonseca@inrae.fr

Citation: M. Guerrero Sanchez, S. Passot, S. Ghorbal, S. Campoy, M. Olivares, F. Fonseca, Insights into the mechanisms of L. salivarius CECT5713 resistance to freeze-dried storage. Cryobiology. 112 (2023) 104556. (DOI:10.1016/j.cryobiol.2023.104556).

Graphical abstract

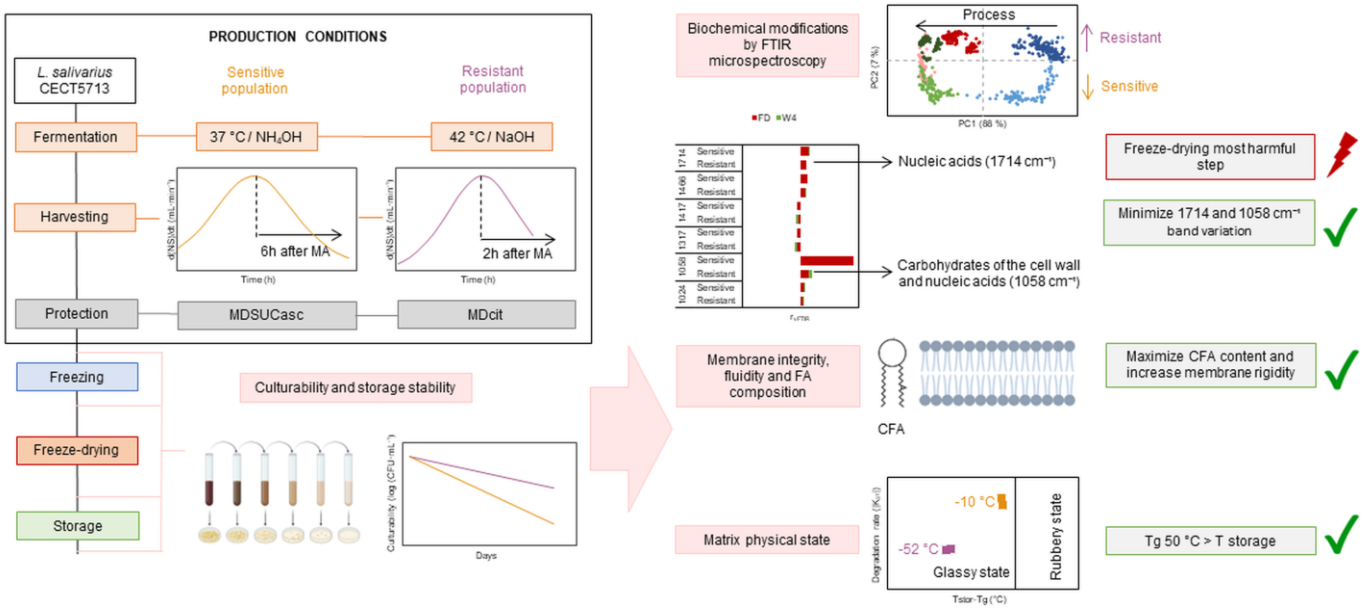

Abstract

Ligilactobacillus salivarius is a lactic acid bacterium exhibiting several health benefits. However, it is sensitive to freeze-drying and storage in the dried state, thus limiting its commercial exploitation. Our objective was to identify markers of cell resistance by applying multiscale characterization to *L. salivarius* CECT5713 cell populations exhibiting different resistance to freeze-dried storage. Cells were produced under two different sets of production conditions differing in the culture parameters (temperature, neutralizing solution, and harvesting time) and the protective formulation composition. The culturability, membrane integrity, and cell biochemical composition assessed by Fourier transform infrared (FTIR) micro-spectroscopy were evaluated after freezing, freeze-drying, and subsequent storage at 37 °C. Membrane properties (fatty acid composition, membrane fluidity, and phospholipid organization), as well as matrix physical properties (glass transition temperature and water activity), were determined. The most resistant cells to freeze-dried storage exhibited the highest cyclic fatty acid content and the most rigid membrane. Freeze-drying and storage induced damage to membrane integrity, proteins, nucleic acids, and constituents of the peptidoglycan cell wall. From the FTIR spectra analysis, we propose the minimization of the variations of the 1058 and 1714 cm^{-1} vibration bands (that arise mainly from symmetric C-O-C stretching and C=O stretching, respectively) induced by the freeze-drying process as a marker of storage stability. We confirmed that a matrix with a glass transition temperature at least 50 °C higher than the storage temperature is crucial for *L. salivarius* CECT5713 storage stability. In addition, this work explored promising FTIR methods for a better understanding of the protection mechanisms involved.

Highlights

- Increasing the cyclic fatty acid content and membrane rigidity correlated with improved freeze-drying and storage resistance
- Two FTIR bands (1058 and 1714 cm^{-1}) associated with other cell components than membrane lipids could be considered preservation markers
- A glassy matrix with a glass transition temperature 50 °C higher than the storage temperature ensured the highest storage stability

Keywords probiotics, lactic acid bacteria, freeze-drying, storage stability, membrane properties, FTIR micro-spectroscopy, glass transition temperature

Introduction

It is well known that the manufacturing, incorporation into food matrices, and commercialization of concentrated lactic acid bacteria (LAB) is not a simple activity and can become a big challenge [9]. The manufacturing of stabilized cell concentrates is a complex process involving several successive operations including fermentation, cooling, concentration, stabilization, and storage. The stabilization, to maximize the shelf life and functional properties of probiotics (e.g., freeze-drying, spray drying), and storage steps induce environmental changes that can generate various types of stress and potential damage on the cells [3, 6, 32]. Among interesting LAB, *Ligilactobacillus salivarius* has been gaining attention in recent years due to the variety of health applications of different strains [4, 26, 29]. The loss of viability and functional properties during the product shelf life leads to under-exploitation of health-beneficial promising *L. salivarius* strains [13].

Different strategies have been reported to minimize cellular damage, reduce the loss of viability and thus improve the LAB resistance to the manufacturing process. Two efficient approaches to improve the resistance to drying and storage processes of LAB in general and *L. salivarius*, in particular, have been noted by different authors: varying culture conditions to expose the cell to moderate stress during fermentation (changing the fermentation temperature, pH, medium culture composition, and harvesting time) and selecting the appropriate protective formulation before the stabilization step (**Table S1**). Improvements in LAB resistance to stabilization processes have been related to several physiological changes such as modulation of the membrane fatty acid (FA) composition, membrane integrity and fluidity, and the synthesis of stress and transport-related proteins (**Table S1**).

However, most of the studies where the production conditions of *L. salivarius* were modified, only assessed their effects on cell growth after fermentation without evaluating them after the freeze-drying and storage processes [13]. In addition, the studies evaluating the survival to drying and storage did not investigate the physiological changes at the origin of improvements observed in the resistance of *L. salivarius* strains [5, 27, 30, 31, 37–39]. To address this lack of knowledge, we have recently studied the effect of protective formulation (mixtures involving maltodextrin, antioxidants, fructooligosaccharides, and trehalose) on the freeze-drying resistance and storage stability of *L. salivarius* CECT5713 [14]. A glassy matrix containing maltodextrin and an antioxidant led to the highest storage stability, thus indicating that the immobilization of cells during storage at temperatures well below the glass transition temperature was essential for strain resistance. Furthermore, FTIR micro-spectroscopic analysis of cells at different process steps revealed that freeze-drying and storage mainly induced damage to proteins, peptidoglycan of the cell wall, and nucleic acids.

In this study, we aimed to apply a deep characterization to *L. salivarius* CECT5713 cells exhibiting different resistance to freeze-drying and storage. The sensitive and resistant *L. salivarius* population were obtained by applying two sets of production conditions differing in the culture conditions and composition of the protective formulation (**Table 1**). We hypothesize that such different populations are worth studying to validate markers of cell preservation found previously and to identify new ones. For this purpose, we characterized and compared the two *L. salivarius* CECT5713 cell populations using a multiscale (matrix, cell membrane, and cell) and multistep (freezing, freeze-drying, and storage) approach. Physical (glass transition temperature and water activity of the matrix), biophysical (membrane integrity, fluidity, and phospholipid organization), and biochemical (FA composition and FTIR features) properties were related

to the biological activity (culturability and storage stability) to identify preservation markers for predicting *L. salivarius* CECT5713 storage stability.

Table 1. Sets of production conditions applied to produce the two *L. salivarius* CECT5713 cell populations investigated

Parameters	**Sensitive population**	**Resistant population**
Pre-culture temperature	37 °C	42 °C
Fermentation temperature	37 °C	42 °C
Neutralizing solution	NH_4OH 25 % (v/v)	NaOH 20 % (v/v)
Harvesting time	6 h after reaching the maximum acidification rate	2 h after reaching the maximum acidification rate
Protective formulation (final concentration in the protected cell concentrate)	Maltodextrin / sucrose / sodium ascorbate (125 / 30 / 10 $g \cdot L^{-1}$)	Maltodextrin / sodium citrate (125 / 10 $g \cdot L^{-1}$)

Maltodextrin (Glucidex IT6, Roquette; Lestrem, France); sodium ascorbate (Royal DSM N.V.; Limburg, Netherland); sodium citrate (Quimivita; Barcelona, Spain); sucrose (Azucarera; Madrid, Spain)

Materials and methods

The experimental approach used in this study is presented in **Figure 1**.

Production and storage conditions of freeze-dried *L. salivarius* CECT5713 concentrates

Ligilactobacillus salivarius CECT5713 was obtained from the Spanish Type Culture Collection (CECT, Valencia, Spain). Two populations exhibiting different resistance to the manufacturing process (sensitive and resistant population) were produced by applying two different sets of production conditions. The resistant *L. salivarius* population was produced according to the procedure described by Guerrero et al. [14]. For the manufacturing of the sensitive population, some production parameters were modified (**Table 1**). Cells were harvested 6 h and 2 h after reaching the maximum acidifying rate (corresponding to the peak of the first derivative curve, **Figure S1**), for the sensitive and resistant populations, respectively. After centrifugation, both cell pellets were diluted with the obtained supernatant and then re-suspended in their corresponding protective solution at a ratio of 3:1 (concentrated cell suspension: protective formulation, v/v). The protected cell concentrates were frozen at -80 °C in sterile Petri dishes. The Petri dishes were then transferred to pre-cooled shelves at -45 °C in a pilot-scale freeze-dryer (VirTis Genesis 35 L SQ EL-85, SP Scientific; Warminster, PA, USA). The shelf temperature value was set between -10 and +10 °C during primary drying and increased to +25 °C for secondary drying. The chamber pressure was set to 0.2 mbar. At the end of the freeze-drying cycle the vacuum was broken and the samples were milled to a powder, packed in aluminium bags, and stored for four weeks at 37 °C.

The whole production process from fermentation to storage was repeated twice (two biological replicates) and three times (three biological replicates) for the sensitive and resistant conditions, respectively. The number of technical replicates (measurements on the same sample) are indicated for each characterization method.

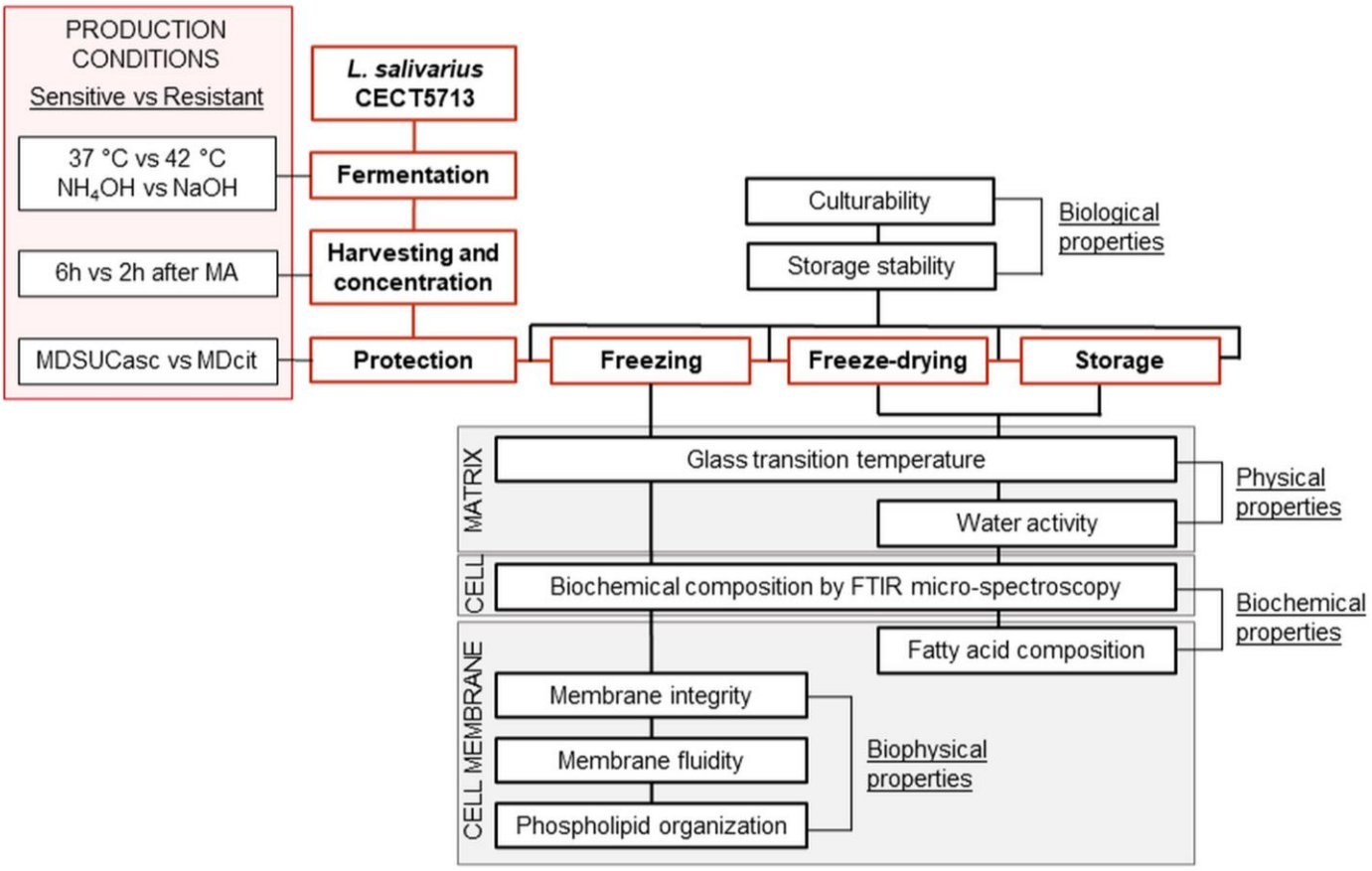

Fig. 1 Diagram of the experimental plan used in this study. It consists of the characterization and comparison of biological, physical, biochemical, and biophysical properties of two *L. salivarius* CECT5713 cell populations with different resistance to the manufacturing process, using a multiscale (matrix, cell, cell membrane) and multistep (freezing, freeze-drying, storage) approach. asc: sodium ascorbate; cit: sodium citrate; FTIR: Fourier transform infrared; MA: maximum acidifying rate; MD: maltodextrin; SUC: sucrose

Biological activity of *L. salivarius* concentrates

Culturability assessment and accelerated storage stability test

Before analysis, frozen samples were thawed at room temperature for 5 min and powder samples were rehydrated in a sterilized solution of 20 g·L^{-1} peptone water (BioMérieux; Marcy l'Étoile, France) and incubated for 30 min at 37 °C with shaking. The amount of peptone water added to the dried sample was calculated to recover the initial water content (77 % (w/w)) of the protected bacterial concentrates (before freeze-drying), from the weight difference between before and after freeze-drying.

Cell culturability was determined using the agar plate count method. Fresh, thawed, or rehydrated cell suspensions were diluted in peptone water and then spread into MRS Agar plates (VWR International Eurolab; Barcelona, Spain). Colonies were enumerated after incubating the plates for 48 h at 37 °C in anaerobic conditions (AnaeroJar™ 2.5 L, Oxoid Ltd.; Basingstoke, Hampshire, England). The cell plate counts were expressed in log (CFU·mL^{-1}). Plate count measurements were performed in triplicate (three technical replicates).

Storage stability was evaluated from the cell loss rate during four weeks of storage at 37 °C, as previously described Guerrero et al. [14]. For each bacterial suspension and biological replicate, the logarithmic value of the cell count (log

(CFU·mL^{-1})) was plotted as a function of the storage time (t, in days). The experimental values were fitted using the following equation (**Eq. 1**):

$$Cell\ count\ (log\ (CFU \cdot mL^{-1})) = -K_{37} \times \mathrm{t\ (days)} + \mathrm{b}$$

Where the cell loss rate constant K_{37} (in days^{-1}) refers to the absolute value of the slope of the linear regression. The lower the absolute value of the slope K_{37}, the higher the storage stability was.

Membrane integrity and esterase activity assessment

Esterase activity was assessed using ChemChrome V8 (BioMérieux; Marcy l'Etoile, France) which contains 21.7 mM carboxyfluorescein diacetate and was associated with lactic acid bacteria viability [8]. Propidium iodide (PI) (Sigma-Aldrich; L'isle d'Abeau, France) (1 mg·mL^{-1} in distilled water), a nucleic acid dye, was used to quantify injured and dead cells. The PI probe can penetrate within cells only when cell membranes have been damaged. Dual staining was performed to differentiate viable (green), dead (red), and injured (double-stained, yellow-orange) cells. Before staining, cell suspensions were diluted in McIlvaine buffer [(citric acid (100 mmol·L^{-1}), disodium hydrogen phosphate dehydrate (Na_2HPO_4, 200 mmol·L^{-1}) adjusted to pH 7.3] to reach approximately 10^6 cells·mL^{-1}. 10 µL of V8 diluted to 1/10 (v/v) in acetone (Sigma Aldrich; Saint Quentin Fallavier, France) and 5 µL of PI were added to 1 mL of the diluted suspension. The mixture was incubated for 10 min at 40 °C before flow cytometry (FCM) analysis with a CyFlow Space cytometer (Sysmex-Partec; Villepinte, France). The FCM analyses were performed according to the method detailed by Bouix and Ghorbal 2017 [2]. Data were collected and analysed with FloMax software (SYSMEX-PARTEC; Villepinte, France) and using statistical tables that indicate numbers and percentages of stained cells determined by each FCM detector, as well as the fluorescence intensity of each fluorescent signal. Flow cytometry measurements were performed in triplicate.

Physical properties of *L. salivarius* concentrates

Glass transition temperature measurements

The glass transition temperature of the freeze-thawed protected cell concentrates (Tg', in °C) and the freeze-dried powders (Tg, in °C) were determined by differential scanning calorimetry (DSC) according to the procedure described by Guerrero et al. [14]. Briefly, measurements were performed on two different power compensation DSC types of equipment (Perkin Elmer LLC, Norwalk, CT, USA): a Diamond equipped with a liquid nitrogen cooling accessory (CryoFill) for the freeze-thawed samples exhibiting thermal events at negative temperatures and a Pyris 1 equipped with a mechanical cooling system (Intracooler 1P) for the powder samples. About 15 – 25 mg of sample was sealed in aluminium pans. Cooling and heating rates of 10 °C·min^{-1} were used. Freeze-thawed samples were scanned following cooling to -100 °C and heating to 20 °C. Powder samples were heated from 10 to 120 – 150 °C, then cooled to 10 °C and heated again to 120 – 150 °C. The first derivative of the heat flow curve was calculated. The glass transition temperature was calculated as the maximal value of the peak observed in the first derivative curve (**Fig. S2**). Measurements were performed in triplicate.

Water activity measurements

The water activity was measured at 25 °C using an a_w meter labMasteraw (Novasina, Precisa, Poissy, France) on freeze-dried samples. Results were obtained from two biological replicates (with no technical replicates).

Cytoplasmic membrane characterization of *L. salivarius* cells

Fatty acid composition

The membrane FA composition of *L. salivarius* cells was determined according to the method detailed by Guerrero et al. [14]. Briefly, a chloroform-methanol 2:1 (v/v) mixture was added to the washed pellet and the mixture was shaken and exposed to ultrasounds. To wash the crude extract, a saline solution (0.15 M NaCl) was added (22 % of crude extract volume) and agitated in a tube rotator (LabRoller™ rotator, Labnet International; NJ, USA). After centrifugation (12.857×g for 15 min at room temperature), the organic (lower) phase was collected and lipids were re-extracted from the remaining aqueous (upper) phase. Both $CHCl_3$ phases were pooled and evaporated by vacuum centrifugation (Jouan RC10.22 vacuum concentrator, Thermo Fisher Scientific; Saint-Herblain, France). The extracted lipids were solubilized in $CHCl_3$, mixed with a C9:0 internal standard (Sigma-Aldrich; St. Louis, MO, USA) and derivatized using trimethylsulfonium hydroxide (TMSH, Sigma-Aldrich; St. Louis, Missouri, USA). FA identification and quantification were carried out using a Hewlett-Packard 6890 gas chromatograph (GMI; Ramsey, MI, USA) coupled to a mass selective detector (5973; Agilent Technologies, Avondale, PA, USA). Results were expressed as FA percentages and obtained from at least two biological replicates (with no technical replicates).

Membrane fluidity

The membrane fluidity of *L. salivarius* was assessed by steady-state fluorescence anisotropy according to the method described by Girardeau et al. [12] with minor modifications. Briefly, 10 µL of 1,6-diphenyl-1,3,5-hexatriene (DPH) fluorescent probe (6 mM, Sigma- Aldrich; St. Louis, MO, USA) prepared in dimethylsulfoxide (DMSO, Sigma-Aldrich; St. Louis, MO, USA) was added to 1 mL of washed bacterial samples (approximately 10^7 cells·mL^{-1} in MES – KOH buffer (50 mM, pH 5.5)). After incubation (3 min in darkness at 35 °C) of the cell suspension, the cell pellet obtained by centrifugation (14.000×g for 90 sec) was re-suspended in 3 mL of a saline solution (0.15 M NaCl) and loaded into a stirred quartz cuvette with a small stirrer. Steady-state fluorescence anisotropy (r) of *L. salivarius* CECT5713 cells was measured in a photoluminescence spectrometer (FLS1000, Edinburgh Instruments, Serlabo Technologies; France). The excitation and emission wavelengths were set at 360 and 430 nm, respectively. Polarizers were located on the excitation source and on the photomultiplier tube to measure anisotropy. Measurements were carried out at different sample temperatures ranging from 45 to 0 °C using a Peltier-based temperature-controlled cuvette holder (LFI-3751, Wavelength electronics; Bozeman, MT, USA), at least in triplicate.

Membrane phospholipid organization

Measurements were carried out on a Nicolet Magna 750 FTIR spectrometer (Thermo Fisher Scientific; Madison, WI, USA) equipped with a mercury/cadmium/telluride (MCT) detector and a variable temperature sample holder (Specac Ldt.; Orpington, Kent, UK), as described by Meneghel et al. [25].

Thawed-protected bacterial samples of *L. salivarius* were centrifuged (13.100×g for 10 min at 4 °C) to obtain a cell pellet. For studying the effect of the protective solution, protected (non-washed) and washed (with saline solution) cell

pellets were investigated. A small amount of the resulting cell pellet was tightly sandwiched between two calcium fluoride (CaF_2) windows (ISP Optics; Riga, Latvia). The windows were inserted into the cell holder and infrared absorption spectra were recorded during cooling from 50 to -50 °C at 2 °C min^{-1}. The spectral acquisition was performed by Omnic software (version 7.1, Thermo Fisher Scientific; Madison, WI, USA). Each acquired spectrum was obtained from 32 co-added scans in the mid-IR region at a 4 cm^{-1} every 45 sec. Spectra analyses were performed using the ASpIR software (Infrared Spectra Acquisition and Processing, INRAE; Palaiseau, France). To determine specific peak locations from each spectrum, second-order derivatives were calculated and smoothed following a 7-point Savitzky-Golay algorithm. The $\nu_s CH_2$ and $\nu_{as} PO_2^-$ peaks, at 2850 and 1220 cm^{-1}, respectively, were plotted as a function of temperature. The $\nu_s CH_2$ plots were fitted with a curve based on an asymmetric sigmoid transition function and the first-order derivative was calculated. Its maximum was taken as the lipid phase transition temperature following freezing (Ts, in °C). Ice nucleation temperature (Tn, in °C) was also determined following the upshift of the combination band of OH libration and bending modes of water (νH_2O). Results were obtained from at least two biological replicates (with no technical replicates).

Biochemical characterization of *L. salivarius* cells

The biochemical characterization of *L. salivarius* protected concentrates in an aqueous environment was carried out at different steps of the stabilization process (after freezing, after freeze-drying, and after four weeks of storage at 37 °C) using an FTIR microscope (Nicolet iN10, Thermo Fisher Scientific; Madison, WI, USA), equipped with a liquid nitrogen-cooled mercury-cadmium-teluride (MCT) detector, and a specific transmission demountable home-made liquid sample holder [26].

Measurements were performed according to the method detailed in Meneghel et al [25] and Guerrero et al [14]. Briefly, freeze-thawed or rehydrated protected cell concentrates were washed three times in saline solution and then centrifuged. A very small amount of the resulting cell pellet was deposited over one side of the CaF_2 microchamber and separated from the diluent side (saline solution) by a thin strip of Mylar® (polyethylene terephthalate film from GoodFellow, Lille). All spectral acquisitions were performed with the Omnic software (version 8.1, Thermo Fisher Scientific; Madison, WI, USA). Each acquired spectrum was obtained from 128 co-added scans in the mid-IR region at a resolution of 4 cm^{-1} every 45 sec. For each bacterial sample, three different sets of spectra were acquired: a background spectrum, sample spectra (at least 60 spectra per biological replicate), and diluent spectra. Spectral pre-processing was performed according to the procedure described by Meneghel et al. [26]. The Omnic software was used for spectral sorting and for removing the residual contribution from water vapour and carbon dioxide to all spectra. The removal of water contributions from all sample spectra was performed using an in-house Matlab script (version 8.3.0.532, Mathworks, Natick; MA, USA) [12, 14, 25] (**Fig. S3**). Post-processing of water subtracted spectra was performed with the Unscrambler® X software package (Version 10.2, CAMO Software AS; Oslo, Norway) on three distinct spectral regions: the 3016 – 2800 cm^{-1}, 1800 – 1370 cm^{-1}, and 1370 – 975 cm^{-1} regions. An extended multiplicative scatter correction (EMSC) procedure was used to normalize and correct the baseline of spectra in each of the spectral regions of interest. The resulting spectra were then statistically analysed by principal component analysis (PCA) to reveal data variance (score plots) and peak positions of interest (loading plots). The assignment of the principal absorption bands was performed using data from the literature on bacteria (**Table S2**). The infrared spectra were further analysed in the

three spectral regions. For each condition set, each step of the process, and biological replicate, the second-order derivative of the average spectrum was calculated (Savitzky-Golay algorithm, third-degree polynomial and a 9-points smoothing factor) (**Fig. 8a**). For each wavenumber (*vi*) corresponding to the peaks observed in the second-order derivative spectra, the relative variation ($r_{v\ FTIR}$) of the peak's height (*h*) compared to the freezing condition was determined as follows (**Eq. 2**):

$$r_{vFTIR} = \frac{h_{viFreeze-drying\ or\ 4\ weeks\ of\ storage}}{h_{viFreezing}} - 1$$

Statistical analyses

To compare data concerning culturability, storage stability, membrane integrity, glass transition temperature, and membrane fluidity, the nonparametric Kruskal-Wallis test and the post-hoc Conover Iman test were performed using XLSTAT 19.6 (Addinsoft; Paris, France) and a significance level of 95 % (p-value < 0.05).

Results

Biological activity of *L. salivarius* CECT5713 populations during stabilization and storage

Culturability and inactivation rate during accelerated storage test

The culturability (concentration of culturable cells) of both *L. salivarius* CECT5713 cell populations were determined after freezing, freeze-drying, and every week for four weeks of storage at 37 °C (**Fig. 2**).

Regardless of the cell population investigated, each step of the manufacturing process, except freezing, produced losses of *L. salivarius* culturability (**Fig. 2**). The decreases in culturability were accentuated as the process progressed. After freeze-drying, *L. salivarius* cells showed a slight reduction of culturability (< -0.8 log units) and no statistical differences were observed between both populations. However, statistical differences appeared throughout storage, with the highest decrease in culturable cell concentration observed in the sensitive population. After four weeks of storage at 37 °C, the culturability after freeze-drying (10.3 log units for both populations) decreased to 3.4 and 7.3 log units for the sensitive and resistant populations, respectively.

Storage stability was evaluated from the inactivation rate constant of *L. salivarius* cell populations after four weeks of storage at 37 °C (K_{37}, in log (CFU·mL^{-1})·day^{-1}) (**Fig. 2b**). K_{37} refers to the value of the linear regression slope determined from the plot of the logarithmic value of the cell count against the storage time. The lower the absolute value of the slope ($|K_{37}|$), the higher the storage stability was. Therefore, the storage stability of the resistant population was significantly improved compared to the sensitive one, as the slope value decreased by about half (0.11 and 0.23 log (CFU·mL^{-1})·day^{-1}, respectively).

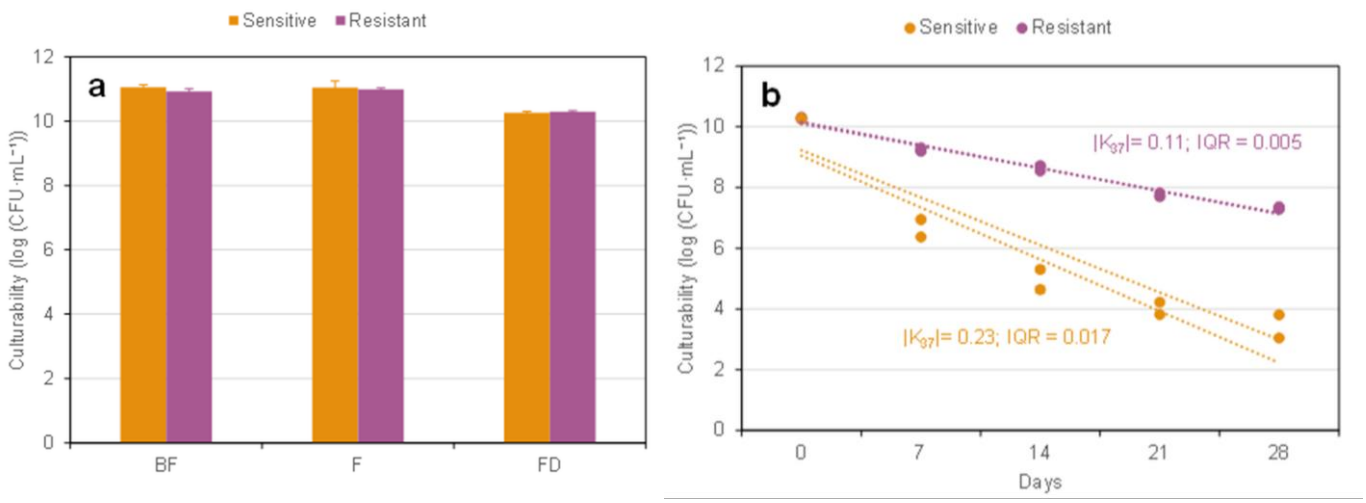

Fig. 2 (**a**) Culturability (log (CFU·mL⁻¹)) of two *L. salivarius* CECT5713 cell populations (sensitive and resistant), at different steps of the manufacturing process: before freezing (BF), after freezing (F), and after freeze-drying (FD). (**b**) Culturability (log (CFU·mL⁻¹)) of two *L. salivarius* CECT5713 cell populations (sensitive and resistant) during 28 days of storage at 37 °C showing the slope value of the linear regression ($|K_{37}|$) determined from **Eq. 1**. Data are the medians of 2-3 biological replicates and at least 3 technical replicates; error bars represent interquartile ranges

Membrane integrity assessment

The membrane integrity was assessed by flow cytometry. The identification of injured and dead cells by PI staining indicated that *L. salivarius* CECT5713 membranes lost integrity and were thus damaged. In freeze-dried cells, the percentage of injured and dead cells increased compared to frozen cells. However, in both populations the percentage of cells with damaged membranes was higher after storage than after freezing and freeze-drying. In addition, statistical differences between both populations were observed. The sensitive cells presented a lower percentage of damaged membranes (15.7 %) than the resistant cells (31.1 %) after freeze-drying, However, after storage, the percentage of injured and dead cells drastically increased (> 69 %) and the resistant cells presented a significant lower percentage of injured and dead cells (69.4 %) than the sensitive cells (93.6 %) (**Fig. 3**).

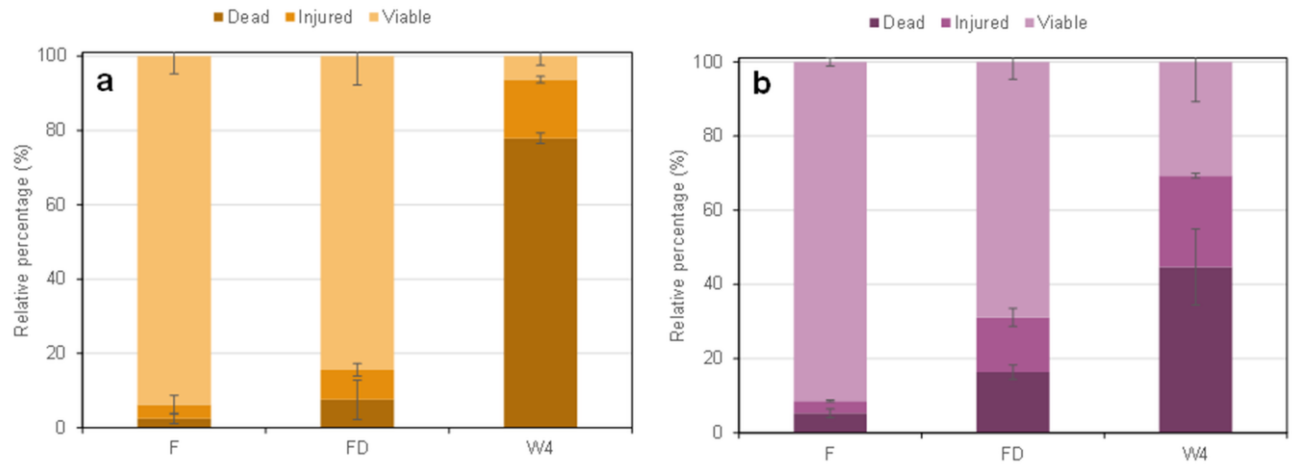

Fig. 3 Evolution of relative percentages of viable, injured, and dead cells of two *L. salivarius* CECT5713 cell populations ((**a**) sensitive and (**b**) resistant) after freezing (F), freeze-drying (FD), and four weeks of storage at 37 °C (W4). The evolution of percentages was evaluated by flow cytometry combined with dual staining (cFDA-PI). Data are the medians of 2-3 biological replicates and at least 3 technical replicates; error bars represent interquartile ranges

Physical properties of the matrices containing *L. salivarius* cell populations

The protected and concentrated cell populations of *L. salivarius* were characterized by measuring the glass transition temperature of the maximally freeze-concentrated phase (Tg'). The glass transition temperature (Tg) and the water activity (aw) of the non-stored freeze-dried powders and those stored for one and four weeks at 37 °C were also determined (**Table 2**).

Table 2. Physical properties (glass transition temperature of bacterial concentrates (Tg') and water activity (aw) and glass transition temperature (Tg) of freeze-dried powders) after freeze-drying (FD), one and four weeks of storage at 37 °C (W1 and W4) of matrices containing *L. salivarius* CECT5713 cell populations (sensitive and resistant)

Population	Tg' (°C)	FD		W1		W4	
		Tg (°C)	aw	Tg (°C)	aw	Tg (°C)	aw
Sensitive	-33.3 [b]	46.0 [b]	0.074	46.8 [b]	0.127	46.5 [b]	0.140
IQR	0.9	2.4	0.016	0.4	0.002	0.9	0.006
Resistant	-29.8 [a]	85.8 [a]	0.030	89.0 [a]	0.043	87.1 [a]	0.103
IQR	0.6	2.0	0.001	2.1	0.000	4.9	0.002

Data presented for Tg' and Tg are medians of 2-3 biological replicates and at least 2 technical replicates; IQR: interquartile ranges. Superscript letters (a, b) represent statistical differences (at the 95 % confidence level) between the two cell populations, at each variable (Tg', Tg) during the process (FD, W1, and W4). Data presented for aw are medians of 2 biological replicates

Both *L. salivarius* cell populations investigated exhibited Tg' and Tg values statistically different. The Tg' was about 3 °C higher for the resistant population than for the sensitive one. Moreover, the Tg value of the freeze-dried matrix of the resistant population was 40 °C higher (86 °C) than that of the sensitive one (46 °C). The Tg values remained relatively constant during the storage and were higher than the storage temperature ($T_{stor.}$ = 37 °C), indicating that freeze-dried samples were stored in a glassy state. The water activity (a_w) values increased during the storage process in both cell populations, being higher for the sensitive one at the three times at which it was measured (after freeze-drying and one and four weeks of storage at 37 °C). Moreover, for the sensitive population, the increase in a_w was most pronounced during the first week of storage.

Cytoplasmic membrane characterization of *L. salivarius* concentrates

Fatty acid composition

The membrane fatty acid composition of *L. salivarius* concentrates produced under the two different production conditions was determined after freeze-drying and four weeks of storage at 37 °C. A total of 12 different FA were detected, identified, and quantified. However, only 7 fatty acids accounted for more than 95 % of the total amount of cell fatty acids: C16:0, C18:0, C18:1 cis 9 and C18:1 cis 11, C19:0 cyc dihydrosterculic, C19:0 cyc phytomonic acid, and C18:2. The percentage of the main groups of FA (UFA: unsaturated FA, SFA: saturated FA, and CFA: cyclic FA) are presented in **Figure 4.** No modifications of the membrane fatty acid composition were detected after storage. However, slight changes between both condition sets in the percentage of some FA were observed (**Fig. 4**). The

membrane of the resistant population presented about 3 % higher content of dihydrosterculic acid (ΔC19:0) (a CFA) and about 1 % lower content of stearic acid (C18:0) than the sensitive one (a SFA).

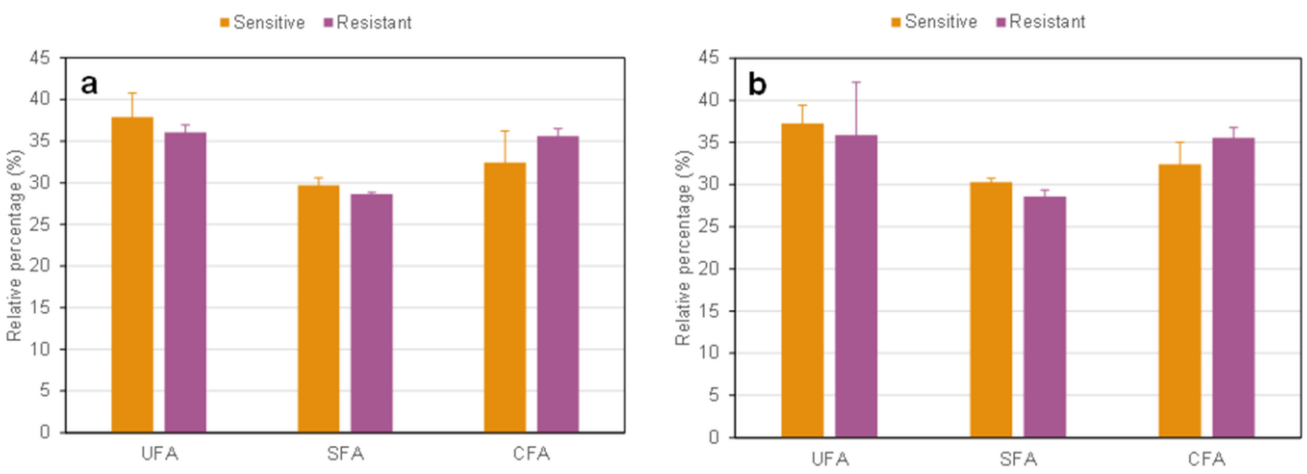

Fig. 4 Fatty acid membrane composition (%) of two *L. salivarius* CECT5713 cell populations (sensitive and resistant) (**a**) after freeze-drying and (**b**) four weeks of storage at 37 °C. Data are the medians of 2-3 biological replicates; error bars represent interquartile ranges. UFA: unsaturated fatty acids; SFA: saturated fatty acids; CFA: cyclic fatty acids

Membrane fluidity

The evolution of membrane fluidity during cooling from 45 to 0 °C of thawed *L. salivarius* concentrates produced under the two different production conditions was assessed by measuring the fluorescence anisotropy of the DPH probe (**Fig. 5**). The higher the anisotropy value, the more rigid the membrane was.

The anisotropy values of washed and labelled cell pellets in a saline solution (0.15 M NaCl) presented a similar variation with temperature regardless of the production condition used (**Fig. 5**). When decreasing the temperature, the anisotropy values and thus the cell membrane rigidity increased. Furthermore, the resistant cell population had a more rigid membrane than the sensitive one (**Fig. 5**) regardless of the temperature value.

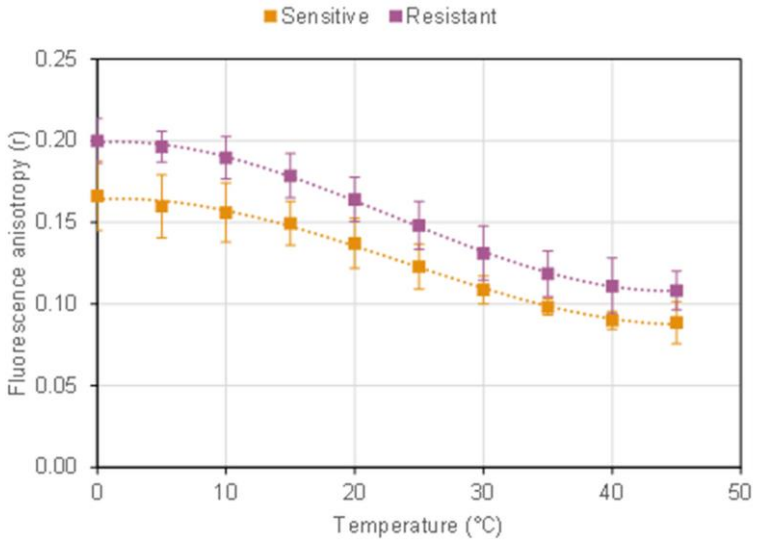

Fig. 5 Evolution of membrane fluorescence anisotropy (r) during cooling of two frozen *L. salivarius* CECT5713 cell populations (sensitive and resistant) in the presence of saline solution. Data are the medians of 2-3 biological replicates and at 5 technical replicates; error bars represent interquartile ranges

Membrane phospholipid organization

The membrane phospholipid organization was evaluated during freezing by FTIR spectroscopy. The behaviour of the $\nu_s CH_2$ band, arising from membrane's phospholipid acyl chains, was modified and shifted to lower frequencies as temperature decreased, regardless of the *L. salivarius* cell population (**Fig. 6a**). No effect of the presence of the protective medium was observed. The first derivative of the $\nu_s CH_2$ curve as a function of temperature was plotted to determine the lipid phase transition (Ts). Ts refers to the transition from a disordered membrane fluid state (liquid-crystalline phase) to an ordered rigid state (gel phase) upon cooling. The resistant population exhibited a Ts value slightly lower than the sensitive one (15 and 21 °C, respectively). In addition, all parameters used to characterize the membrane lipid transition of *L. salivarius* CECT5713 cells with the $\nu_s CH_2$ band, presented similar values for the two cell populations in the presence and absence of the protective medium.

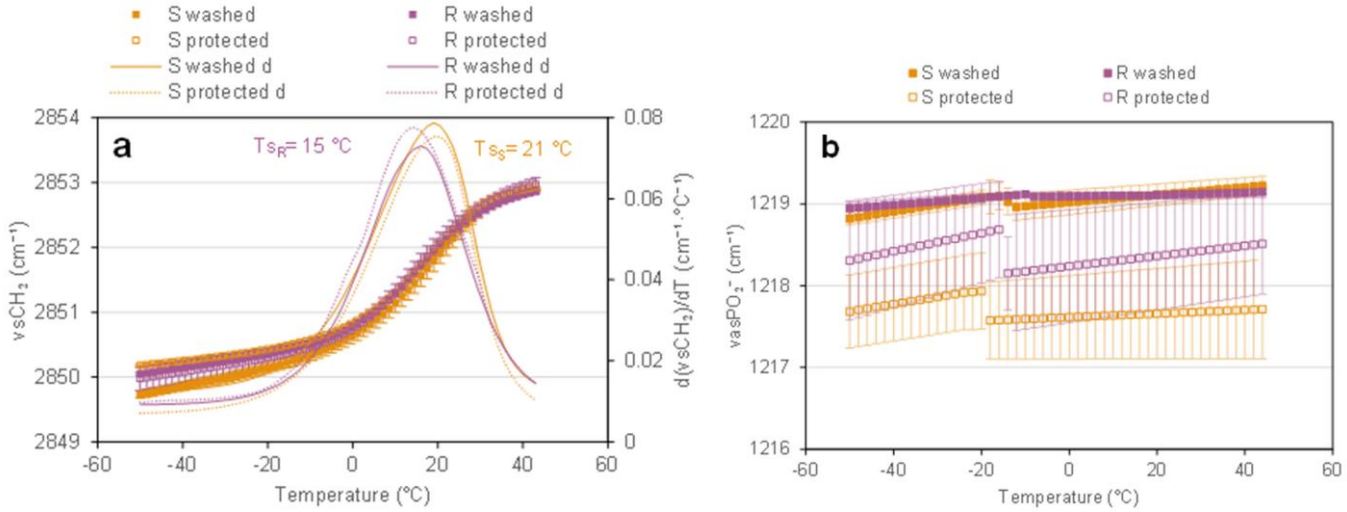

Fig. 6 (**a**) Peak positions of the symmetric CH_2 stretching vibration band ($\nu_s CH_2$) during cooling of two *L. salivarius* CECT5713 cell populations (S, sensitive and R, resistant) in the presence of protective formulations (□ and ---) and washed with saline solution (■ and —). Lines indicate the first derivative of the $\nu_s CH_2$ band and the maximum of each one corresponds to the lipid transition temperature (Ts) from a liquid-crystalline to a gel phase. (**b**) Peak positions of the asymmetric PO_2^- stretching vibration band ($\nu_{as}PO_2^-$) during cooling of two *L. salivarius* CECT5713 cell populations (S, sensitive and R, resistant) in the presence of protective formulation (□) and washed with saline solution (■). Data are the medians of 2-3 biological replicates; error bars represent interquartile ranges

The vibration of the PO_2^- group can be associated with the phosphate moiety of phospholipid headgroups of the bilayer, teichoic acids present in the cell wall, or nucleic acid structures. However, since the behavior of the $\nu_{as}PO_2^-$ band in LAB was reported to be directly affected by the drying [7, 36] or the ice nucleation during freezing [24], the vibration of the PO_2^- group has been attributed to macromolecules that are directly in contact with the extracellular medium, thus excluding nucleic acids and other intracellular phosphorylated molecules. **Figure 6b** displayed the behaviour of the $\nu_{as}PO_2^-$ band as a function of temperature for both populations in saline solution and the protective medium. In the presence of saline solution (filled squares), a similar $\nu_{as}PO_2^-$ band behaviour with temperature was observed for both cell populations (constant value of frequencies around 1219 cm^{-1}). The presence of the protective medium (open squares) led to a decrease in the band frequency for the whole temperature range. This decrease was more pronounced for the sensitive population (orange open squares) than for the resistant one. Moreover, a frequency shift was observed when ice nucleation occurred in protected cell concentrates (an increase of around 0.4 cm^{-1}).

Biochemical composition after freeze-drying and four weeks of storage of *L. salivarius* cells

Principal component analyses (PCA) were performed on normalized and EMSC-corrected spectra of *L. salivarius* cell populations (sensitive and resistant population) acquired after freezing, freeze-drying, and four weeks of storage at 37 °C, in three different mid-IR spectral regions: 3016 – 2800 cm^{-1}, 1800 – 1370 cm^{-1}, and 1370 – 975 cm^{-1}. The main vibrational bands identified in the loading plots were assigned to cellular components according to the literature (**Table S2**).

The PC1 versus PC2 score plots and the corresponding PC1 and PC2 loading plots in the 1800 – 1370 cm^{-1} and 1370 – 975 cm^{-1} regions are reported in **Figure 7**. Regardless of the spectral region and the *L. salivarius* cell population, the cluster of frozen cells was separated from the clusters of freeze-dried and stored cells along PC1 (88 and 78 % of the total variance, respectively). However, the cluster of frozen cells of the sensitive population exhibited a higher dispersion along the PC1 axis than the resistant one (**Fig. 7a** and **b**). The clusters of freeze-dried and stored cells of the sensitive population overlapped, while those of the resistant population were slightly separated, the freeze-dried spectra being located between frozen and stored spectra along PC1.

The positive peaks in the loading plots of PC1 (**Fig. 7c** and **d**) revealed that the frozen cells were characterized by two spectral features in the 1620 – 1560 cm^{-1} and 1135 – 1065 cm^{-1} ranges. The negative peaks in the loading plots of PC1 revealed that the stored cells of both populations and freeze-dried cells of the sensitive population were characterized by six spectral features in the 1760 – 1720 cm^{-1}, 1670 – 1655 cm^{-1}, 1550 – 1430 cm^{-1}, 1300 – 1260 cm^{-1}, 1165 – 1150 cm^{-1}, and 1055 – 1000 cm^{-1} ranges.

For both spectral regions (1800 – 1370 cm^{-1} and 1370 – 975 cm^{-1}), the clusters of frozen, freeze-dried, and stored cells of the resistant population were separated from the frozen and stored cells of the sensitive population along PC2 (7 and 14% of the total variance, respectively). The positive peaks in the loading plots of PC2 (**Fig. 7e** and **f**) revealed that the cells of the resistant population were characterized by spectral features in the 1720 – 1680 cm^{-1} and 1255 – 1210 cm^{-1} ranges. Conversely, the cells of the sensitive population were characterized by three negative peaks in the PC2 loading plots in the 1560 – 1550 cm^{-1}, 1330 – 1305 $cm^{-,1}$ and 1150 – 1135 cm^{-1} ranges.

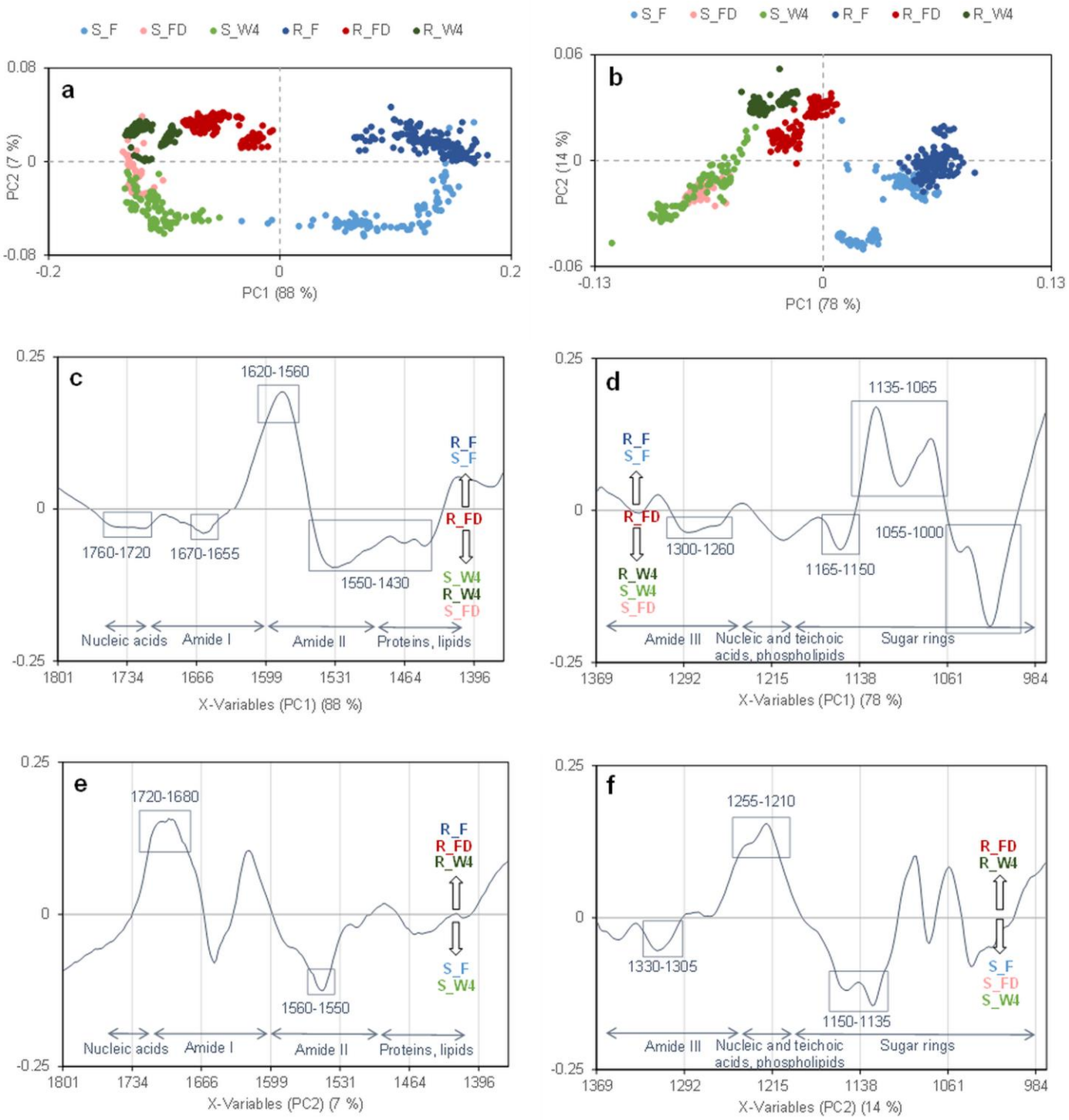

Fig. 7 Principal component analysis (PCA) of FTIR normalized and corrected spectra of frozen (F), freeze-dried (FD), and stored (W4) of two *L. salivarius* CECT5713 cell populations (S, sensitive and R, resistant) in an aqueous environment in the (**a, c, e**) 1800 – 1370 cm^{-1} and (**b, d, f**) 1370 – 975 cm^{-1} region. (**a**) PC1 versus PC2 score plots explain 88 and 7 % of the variance, respectively. (**b**) PC1 versus PC2 score plots explain 78 and 14 % of the variance, respectively. (**c, d**) Loading plots of the PC1: positive peaks characterized the frozen cells, whereas negative peaks characterized the stored cells of both populations and freeze-dried cells of the sensitive population. (**e, f**) Loading plots of the PC2: positive peaks characterized the cells of the resistant population, whereas negative peaks characterized the cells of the sensitive population

In the 3016 – 2800 cm^{-1} spectral region, containing information on fatty acyl chains of the bacterial membranes, slight separations associated with the processes or the production conditions of cell populations were observed in the score plot, along PC2 (**Fig. S4**). The second derivatives of the averaged spectra of the frozen sensitive and resistant populations

were examined (**Fig. S4d**), and a peak at approximately 2987 cm^{-1} allowed the discrimination of both populations. This peak has been associated with cyclic fatty acids by Kochan et al. [17].

To get further insight into the biochemical modification induced by freeze-drying and storage on both *L. salivarius* cell populations, the second order derivative of the averaged spectra was plotted in the spectral region of 3016 – 975 cm^{-1} for each population and process step (**Fig. 8a**). The relative variation of the peak's height compared to the frozen populations ($r_{v\ FTIR}$) was calculated. The assignment of the main vibrational bands identified in the second-order derivative, as well as the qualitative change induced by the process step, are summarized in **Table S2**. In **Figure 8b** are represented the infrared vibrational bands that displayed the biggest changes (increasing or decreasing > 0.5 in the $r_{v\ FTIR}$). A positive value means that the freeze-drying or the storage, resulted in increasing the peak height compared to freezing. The main changes in the infrared vibrational bands were observed after the freeze-drying step regardless of the cell population. The storage for four weeks at 37 °C only intensified them. The freeze-drying process led to an increase in the $r_{v\ FTIR}$ (+0.50 to +7.22) at the following infrared vibration bands: 1714 cm^{-1} (nucleic acids), 1466 cm^{-1} (proteins, lipids), 1058 cm^{-1} (carbohydrates, nucleic acids), and 1024 cm^{-1} (carbohydrates); and decreased these others: 1417 cm^{-1} (carbohydrates, proteins, nucleic acids, lipids) and 1317 cm^{-1} (proteins). For both populations, but especially for the sensitive one, the highest increase was observed in the 1058 cm^{-1} band ($r_{v\ FTIR}$ = +7.22).

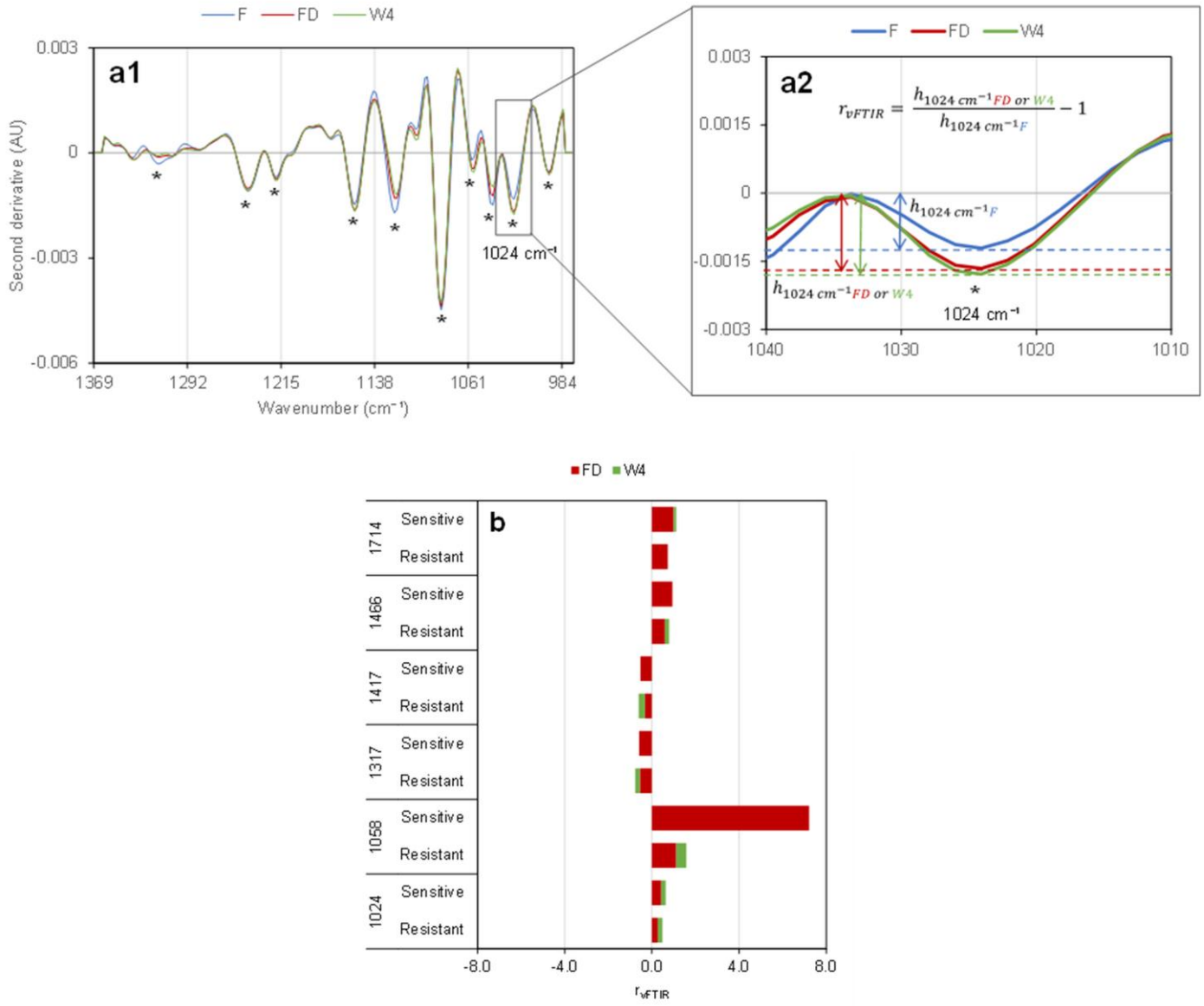

Fig. 8 (**a**) Method used to further analyse the spectra of *L. salivarius* CECT5713 cell populations. (**a1**) Mean second derivative of the normalized spectrum of the frozen (F), freeze-dried (FD), and stored for four weeks at 37 °C (W4) sensitive cells on the 1370 – 975 cm^{-1} region, showing the peaks where the effect of the conditions has been evaluated. (**a2**) Zoom on the 1040 – 1010 cm^{-1} region showing how the relative variation (r_{vFTIR}) of the 1024 cm^{-1} peak's height in the freeze-dried ($h_{1024\,cm^{-1}FD}$) and stored for four weeks at 37 °C ($h_{1024\,cm^{-1}W4}$) compared to the frozen ($h_{1024\,cm^{-1}F}$) sample is calculated. (**b**) Main changes observed in the relative variation (r_{vFTIR}) of the infrared vibrational bands in the 1800 – 975 cm^{-1} region in the *L. salivarius* CECT5713 freeze-dried (FD) and stored for four weeks at 37 °C (W4) cell populations (sensitive and resistant), compared to their corresponding frozen sample

Discussion

Drawing on recent research on the preservation of *L. salivarius* CECT5713 [14], the present article aimed to identify properties of the cells and protective matrix that could be related to the improvement of freeze-dried storage stability. By applying physical, biochemical, and biophysical characterization techniques to compare two cell populations exhibiting different resistance to freeze-dried storage, it was possible to identify the main damaged components of *L. salivarius* CECT5713 cells and propose new markers of cell preservation. This study has revealed quantitative data about the harmful effects of freeze-drying and storage on the cell membrane integrity and other cell components (proteins, peptidoglycan of the cell wall, and nucleic acids). Additionally, our results highlighted that cell properties

such as fatty acid composition and membrane fluidity, originated in the fermentation step, led to improved bacterial preservation. The present results also confirmed the crucial role of a protective glassy matrix with a glass transition temperature at least 50 °C higher than the storage temperature (afforded by a polymer such as maltodextrin) to increase freeze-dried storage stability.

The cell membrane of LAB is often reported as a major target of cell damage during stabilization processes due to its location between the extracellular and intracellular medium. LAB membrane damage was demonstrated by significant losses of LAB membrane integrity after freeze-drying [35] and storage [23]. In agreement with these previous works, the membrane integrity of *L. salivarius* CECT5713, quantified in this work for the first time, was affected by freeze-drying and accelerated storage (**Fig. 3**). Since the lipid composition did not significantly change during storage (**Fig. S4**), our findings confirm that alternative mechanisms than membrane lipid oxidation need to be considered to explain the membrane integrity and culturability losses observed following freeze-dried storage [15, 35]. Other cellular components of *L. salivarius* CECT5713 were also affected by freeze-drying and storage. In agreement with previous work on the protection of *L. salivarius* CECT5713 [14], the slight loss of culturability during freeze-drying and the drastic loss during storage at 37 °C were associated with damage to proteins, nucleic acids, and peptidoglycans of the cell wall (**Fig. 7**). Although several infrared spectral bands were modified in this work in the 1800 – 975 cm^{-1} region for both sensitive and resistant cells, the main change was observed for the 1058 cm^{-1} band and, to a lesser extent, for the 1714 cm^{-1} band (**Fig. 8b**). The modifications of these two bands were related to the worst *L. salivarius* CECT5713 resistance to freeze-drying and storage. The 1058 cm^{-1} band has been associated with several cell compounds (carbohydrates of the cell wall and nucleic acids), while the 1714 cm^{-1} has been assigned to the nucleic acids (**Table S2**). Both bands, when unchanged, appear as potential markers of *L. salivarius* CECT5713 cell preservation.

The biochemical and biophysical properties of generated following the fermentation step have been related to the cell resistance to the freeze-drying and storage processes (**Table S1**). The fatty acid composition modification, especially an increase in the CFA content, has been associated with improved LAB survival after freeze-dried storage. Although it has been little studied [35], is confirmed by our results. The content of CFA in LAB membranes is mainly governed by the fermentation conditions and the LAB species and strains. The fermentation temperature and harvesting time have previously been reported to increase the CFA content [16, 19, 35]. Increasing the CFA content affects the biophysical properties of the membrane, which tends to rigidify. This homeoviscous adaptation was also observed for *L. lactis* TOMSC161, increasing fermentation temperature and harvesting in the stationary phase led to an increased concentration of CFA and SFA and membrane rigidity. The exact function of CFA in cell preservation is still unclear. Some authors have hypothesized that CFA have the same physical properties as UFA and therefore, increase membrane fluidity by preventing the phospholipids packing [10, 22, 40]. Our results however, converge with other studies showing that CFA decrease membrane fluidity by restricting the mobility and disorder of the phospholipids bilayer [19, 21, 28, 35]. Furthermore, the fermentation conditions induced additional cellular modifications than the changes in membrane fatty acid composition. It was demonstrated that the synthesis of specific proteins during fermentation resulted in improving LAB freeze-drying resistance (**Table S1**). In agreement with the literature, both populations of *L. salivarius* were differentiated according to proteins' infrared features (**Fig. 7a, c** and **e**).

The protective formulation is another factor that can modulate the effect of the membrane composition on the biophysical properties and final resistance to freeze-drying and storage. Protective molecules did not induce clear-cut modifications on the properties of the membrane core ($\nu_s CH_2$ behavior, **Fig. 6a**) in agreement with previous work on *L. lactis* TOMSC161 [35]. However, the protective formulation modified the interaction between the membranes' surface and the environment ($\nu_{as}PO_2^-$) (**Fig. 6b**). The position of the $\nu_{as}PO_2^-$ band informs about the hydrogen bonding state of the phospholipid headgroups and the interactions between protective molecules and the phospholipid headgroups [18, 20]. The shift of the band to lower frequency values indicates an increase in the hydrogen bonding interactions around the phospholipid headgroups and a decrease in the phospholipid headgroups packing [11, 36]. According to that, the addition of protective molecules to *L. salivarius* cells indicated that the phospholipid headgroups of the most resistant cell membranes could have less interaction with the extracellular medium and thus, be more tightly packed than those of the sensitive cells. These results offer a promising perspective for studying the LAB formulation step (e.g., protective molecules, strains) to fully understand the information given by the $\nu_{as}PO_2^-$ band and the implications in the protective mechanisms.

Finally, the protective molecules provided an amorphous glassy matrix whose high viscosity could slow down main deterioration reactions [1, 34]. The Tg of the bacterial concentrates indicated that both *L. salivarius* cell populations were stored in a glassy state (Tg > Tstor, **Table 2**). As shown in **Figure 9a**, the storage stability of *L. salivarius* freeze-dried samples decreased when approaching the rubbery state. Consequently, the sensitive cells were the closest to this state (Tstor-Tg = -10 °C), while resistant cells showed the greatest distance to the rubbery state (Tstor-Tg = -52 °C) and thus, the best storage stability ($|K_{37}| = 0.11$). Our findings are in agreement with previous results [14] also presented in **Figure 9a**. When considering the sensitive *L. salivarius* population, the positive effect of the antioxidant sodium ascorbate that was previously observed on *L. salivarius* survival after storage [14] seems not to be enough to compensate for the negative impact of the different culture conditions and the sucrose addition, which significantly decreases the glass transition temperature. The principal parameter affecting Tg is the water content [1], which together with the protective compounds determines the water activity of samples. However, the best storage stability of *L. salivarius* was obtained when the water activity was less than 0.05 after the freeze-drying step and about 0.1 after four weeks of storage at 37 °C (**Fig. 9b**).

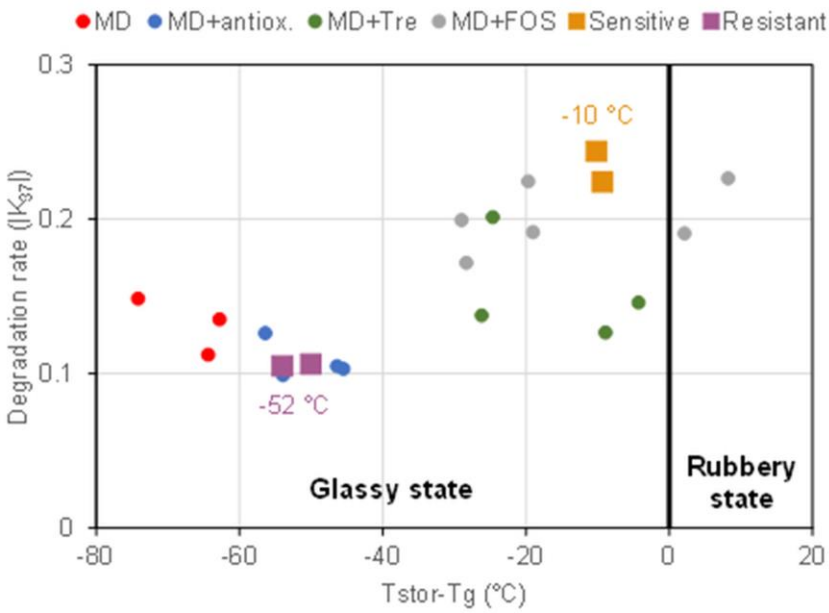

Fig. 9 (**a**) Relationship between the inactivation rate during storage ($|K_{37}|$) of two *L. salivarius* CECT5713 cell populations (sensitive and resistant) and the difference between the storage temperature (Tstor. = 37 °C) and the glass transition temperature of the freeze-dried samples (Tg) (Tstor-Tg, in °C). (**b**) Relationship between the inactivation rate during storage ($|K_{37}|$) of two *L. salivarius* CECT5713 cell populations (sensitive and resistant) and their water activity after freeze-drying (aw at FD). Some of the data were taken from Guerrero et al.[14]. antiox.: antioxidant molecule; FOS: fructooligosaccharide; MD: maltodextrin; Tre: trehalose

The differences between the two sets allowed us to propose relationships between biological responses and cellular changes but prevented us from unequivocally relating them to the factors causing these changes. However, in our study, we have focused on the implementation of different methods at different scales to characterize the properties of cells exhibiting significantly different resistance to the stabilization processes, and such different cell states often arise from multifactor modifications.

Conclusions

This work focused on the characterization and comparison of two *L. salivarius* CECT5713 populations, produced under two sets of production conditions differing in the culture parameters and protective formulation, and exhibiting different levels of resistance to freeze-dried storage for four weeks at 37 °C. The differences in the biological activity (culturability, and storage stability) between the sensitive and the resistant cell population were related to the membrane properties (FA composition, membrane fluidity, and phospholipid organization) and other cell components modifications (membrane integrity, nucleic acids, proteins, and peptidoglycans of the cell wall), as well as the physical properties of the freeze-dried matrix. Comparing the changes produced in these properties between both populations, using a multiscale (matrix, cell membrane, and cell) and multistep (freezing, freeze-drying, and storage) approach, helped us to identify and propose markers of preservation for *L. salivarius* CECT5713 (**Table 3**). We tried to classify these markers considering whether they are determined by the fermentation conditions, the protective molecules, or potentially by both of them. In the future, applying a similar approach to other *L. salivarius* CECT5713 populations produced in different production conditions, or other LAB could help us to confirm the suggested preservation markers and propose generalized mechanisms of protection. Moreover, FTIR micro-spectroscopy appears as a powerful tool for screening production conditions leading to long-term storage stability of freeze-dried probiotic microorganisms.

Table 3. Summary of the proposed markers of *L. salivarius* CECT5713 resistance to freeze-drying and storage, according to the property measured and the stage of the manufacturing process that determines it

Stage	Property	Marker of resistance
Fermentation	Membrane composition	Maximize CFA content
	Membrane anisotropy	Increase in membrane rigidity
	Biophysical property of the membrane: lipid phase transition ($\nu_s CH_2$, FTIR)	More studies are required to clarify the effect
Protection	Matrix	Tg at least 50 °C higher than the storage temperature
	Biophysical property of the membrane ($\nu_{as} PO_2^-$, FTIR)	Modification of the hydrogen bonding interaction and headgroup packing (more studies required to define the effect)
Fermentation and protection	Biochemical composition of cells (FTIR micro-spectroscopy)	Modification of the nucleic acid, protein and constituents of the peptidoglycan cell wall. Minimize the variation of the 1714 and 1058 cm^{-1} bands

CFA: cyclic fatty acids; FTIR: Fourier transform infrared; Tg: glass transition temperature

Data availability

The datasets generated during and/or analysed during the current study are available in the Data INRAE repository, https://doi.org/10.57745/AJO9FD

Authors' contribution

Conceptualization and methodology MGS, SP, FF; experiments MGS (SG for flow cytometry measurements, FF for anisotropy measurements); formal analysis MGS, FF; data curation and statistical treatment MGS, SG, SP, FF; writing original draft of the paper and writing review MGS, SP, FF; final review and editing MGS, SP, FF, SG, SC, MO; supervision and project administration FF, SP, SC, MO; resources and funding acquisition FF, SP, SC, MO.

Acknowledgments

We thank Pascale Lieben from INRAE and Anne-Claire Peron from AgroParisTech for training MGS to FTIR spectroscopy and fatty acid composition analysis, respectively. Finally, we thank Cristina Diaz Morillo from Biosearch S.A.U (a Kerry® company) for her implication in the management and coordination of the European project PREMIUM RISE (N° 777657).

Funding: This work has received funding from the European Union's Horizon 2020 research and innovation program under grant agreement N° 777657.

Compliance with Ethical Standards

Conflict of interest: The authors declare that they have no conflict of interest.

Ethical approval: This article does not contain any studies with human participants or animals performed by any of the authors.

References

[1] M. Aschenbrenner, U. Kulozik, P. Foerst P, Evaluation of the relevance of the glassy state as stability criterion for freeze-dried bacteria by application of the Arrhenius and WLF model, Cryobiology. 65 (2012) 308–318. https://doi.org/10.1016/j.cryobiol.2012.08.005.

[2] M. Bouix, S. Ghorbal, Assessment of bacterial membrane fluidity by flow cytometry, J. Microbiol. Methods. 143 (2017) 50–57. https://doi.org/10.1016/j.mimet.2017.10.005.

[3] G. Broeckx, D. Vandenheuvel, I.J.J. Claes, S. Lebeer, F. Kiekens F, Drying techniques of probiotic bacteria as an important step towards the development of novel pharmabiotics, Int. J. Pharm. 505 (2016) 303–318. https://doi.org/10.1016/j.ijpharm.2016.04.002.

[4] B.D. Chaves, M.M. Brashears, K.K. Nightingale KK, Applications and safety considerations of *Lactobacillus salivarius* as a probiotic in animal and human health, J. Appl. Microbiol. 123 (2017) 18–28. https://doi.org/10.1111/jam.13438.

[5] B.M. Corcoran, R.P. Ross, G.F. Fitzgerald, C. Stanto, Comparative survival of probiotic lactobacilli spray-dried in the presence of prebiotic substances, J. Appl. Microbiol. 96 (2004) 1024–1039. https://doi.org/10.1111/j.1365-2672.2004.02219.x.

[6] M. Cunningham, G. Vinderola, D. Charalampopoulos, S. Lebeer, M.E. Sander, R. Grimaldi R, Applying probiotics and prebiotics in new delivery formats – is the clinical evidence transferable?, Trends Food Sci. Technol. 112 (2021) 495–506. https://doi.org/10.1016/j.tifs.2021.04.009.

[7] D. Dianawati, V. Mishra, N.P. Shah, Role of calcium alginate and mannitol in protecting Bifidobacterium, Appl. Environ. Microbiol. 78 (2012) 6914–6921. https://doi.org/10.1128/AEM.01724-12.

[8] A. El Arbi, S. Ghorbal, A. Delacroix-Buchet, M. Bouix, Assessment of the dynamics of the physiological states of *Lactococcus lactis* ssp. *cremoris* SK11 during growth by flow cytometry: Dynamics of the physiological states of *L. lactis* ssp. *cremoris*, J. Appl. Microbiol. 111 (2011) 1205–1211. https://doi.org/10.1111/j.1365-2672.2011.05114.x.

[9] K. Fenster, B. Freeburg, C. Hollard, C. Wong, R. Rønhave Laursen, A. Ouwehand, The production and delivery of probiotics: a review of a practical approach, Microorganisms. 7 (2019) 83. https://doi.org/10.3390/microorganisms7030083.

[10] F. Fonseca, C. Pénicaud, E.E. Tymczyszyn, A. Gómez-Zavaglia, S. Passot, Factors influencing the membrane fluidity and the impact on production of lactic acid bacteria starters, Appl. Microbiol. Biotechnol. 103 (2019) 6867–6883. https://doi.org/10.1007/s00253-019-10002-1.

[11] M.A. Frías, S.B. Díaz, N.M. Ale, A. Ben Altabef, E.A. Disalvo, FTIR analysis of the interaction of arbutin with dimyristoyl phosphatidylcholine in anhydrous and hydrated states, Biochim. Biophys. Acta BBA - Biomembr. 1758 (2006) 1823–1829. https://doi.org/10.1016/j.bbamem.2006.06.024.

[12] A. Girardeau, S. Passot, J. Meneghel, S. Cenard, P. Lieben, I.C. Trelea, F. Fonseca, Insights into lactic acid bacteria cryoresistance using FTIR microspectroscopy, Anal. Bioanal. Chem. 414 (2022) 1425–1443. https://doi.org/10.1007/s00216-021-03774-x.

[13] M. Guerrero Sanchez, S. Passot, S. Campoy, M. Olivares, F. Fonseca, *Ligilactobacillus salivarius* functionalities, applications, and manufacturing challenges, Appl. Microbiol. Biotechnol. 106 (2022) 57–80. https://doi.org/10.1007/s00253-021-11694-0.

[14] M. Guerrero Sanchez, S. Passot, S. Campoy, M. Olivares, F. Fonseca, Effect of protective agents on the storage stability of freeze-dried *Ligilactobacillus salivarius* CECT5713, Appl. Microbiol. Biotechnol. 106 (2022) 7235–7249. https://doi.org/10.1007/s00253-022-12201-9.

[15] M.L.R.W. Hansen, M.A. Petersen, J. Risbo, M. Hümmer, A. Clausen, Implications of modifying membrane fatty acid composition on membrane oxidation, integrity, and storage viability of freeze-dried probiotic, *Lactobacillus acidophilus* La5, Biotechnol. Prog. 31 (2015) 799–807. https://doi.org/10.1002/btpr.2074.

[16] L. Hua, Z. WenYing, W. Hua, L. ZhongChao, W. AiLian, Influence of culture pH on freeze-drying viability of *Oenococcus oeni* and its relationship with fatty acid composition, Food Bioprod. Process. 87 (2009) 56–61. https://doi.org/10.1016/j.fbp.2008.06.001.

[17] K. Kochan, H. Peng, E.S.H. Gwee, E. Izgorodina, V. Haritos, B.R. Wood, Raman spectroscopy as a tool for tracking cyclopropane fatty acids in genetically engineered Saccharomyces cerevisiae, The Analyst. 144 (2019) 901–912. https://doi.org/10.1039/C8AN01477A.

[18] R.N.A.H. Lewis, R.N. McElhaney, The structure and organization of phospholipid bilayers as revealed by infrared spectroscopy, Chem. Phys. Lipids. 96 (1998) 9–21. https://doi.org/10.1016/S0009-3084(98)00077-2.

[19] C. Li, J.L. Zhao, Y.T. Wang, X. Han, N. Liu, Synthesis of cyclopropane fatty acid and its effect on freeze-drying survival of *Lactobacillus bulgaricus* L2 at different growth conditions, World J. Microbiol. Biotechnol. 25 (2009) 1659–1665. https://doi.org/10.1007/s11274-009-0060-0.

[20] L.J.M. Linders, W.F. Wolkers, F.A. Hoekstra, K. van 't Riet, Effect of added carbohydrates on membrane phase behavior and survival of dried *Lactobacillus plantarum*, Cryobiology. 35 (1997) 31–40. https://doi.org/10.1006/cryo.1997.2021.

[21] N. Loffhagen, C. Härtig, W. Geyer, M. Voyevoda, H. Harms, Competition between cis, trans and cyclopropane fatty acid formation and its impact on membrane fluidity, Eng. Life Sci. 7 (2007) 67–74. https://doi.org/10.1002/elsc.200620168.

[22] M.C. Machado, C.S. López, H. Heras, E.A. Rivas, Osmotic response in *Lactobacillus casei* ATCC 393: biochemical and biophysical characteristics of membrane, Arch. Biochem. Biophys. 422 (2004) 61–70. https://doi.org/10.1016/j.abb.2003.11.001.

[23] I. Meireles Mafaldo, V. de Medeiros, W. da Costa, C. da Costa Sassi, M. da Costa Lima, E. de Souza, C. Eduardo Barão, T. Colombo Pimentel, M. Magnani, Survival during long-term storage, membrane integrity, and ultrastructural aspects of Lactobacillus acidophilus 05 and *Lacticaseibacillus casei* 01 freeze-dried with freshwater microalgae biomasses, Food Res. Int. 159 (2022) 111620. https://doi.org/10.1016/j.foodres.2022.111620.

[24] J. Meneghel, S. Passot, S. Dupont, F. Fonseca, Biophysical characterization of the *Lactobacillus delbrueckii* subsp. *bulgaricus* membrane during cold and osmotic stress and its relevance for cryopreservation, Appl. Microbiol. Biotechnol. 101 (2017) 1427–1441. https://doi.org/10.1007/s00253-016-7935-4.

[25] J. Meneghel, S. Passot, F. Jamme, S. Lefrançois, P. Lieben, P. Dumas, F. Fonseca, FTIR micro spectroscopy using synchrotron-based and thermal source-based radiation for probing live bacteria, Anal. Bioanal. Chem. 412 (2020) 7049–7061. https://doi.org/10.1007/s00216-020-02835-x.

[26] S. Messaoudi, M. Manai, G. Kergourlay, H. Prévost, N. Connil, J. Chobert, X. Dousset, *Lactobacillus salivarius*: bacteriocin and probiotic activity, Food Microbiol. 36 (2013) 296–304. https://doi.org/10.1016/j.fm.2013.05.010.

[27] L.C. Ming, R.A. Rahim, H.Y. Wan, A.B. Ariff, Formulation of protective agents for improvement of *Lactobacillus salivarius* I24 survival rate subjected to freeze-drying for production of live cells in powderized form, Food Bioprocess Technol. 2 (2009) 431–436. https://doi.org/10.1007/s11947-009-0184-0.

[28] J. Muñoz-Rojas, P. Bernal, E. Duque, P. Godoy, A. Segura, J. Ramos, Involvement of cyclopropane fatty acids in the response of Pseudomonas putida KT2440 to freeze-drying, Appl. Environ. Microbiol. 72 (2006) 472–477. https://doi.org/10.1128/AEM.72.1.472-477.2006.

[29] B. Neville, P. O'Toole, Probiotic properties of *Lactobacillus salivarius* and closely related *Lactobacillus* species, Future Microbiol. 5 (2010) 759–774. https://doi.org/10.2217/fmb.10.35.

[30] K.B.P.K. Reddy, S.P. Awasthi, A.N. Madhu, S.G. Prapulla, Role of cryoprotectants on the viability and functional properties of probiotic lactic acid bacteria during freeze-drying, Food Biotechnol. 23 (2009) 243– 265. https://doi.org/10.1080/08905430903106811.

[31] K.B.P.K. Reddy, A.N. Madhu, S.G. Prapulla, Comparative survival and evaluation of functional probiotic properties of spray-dried lactic acid bacteria, Int. J. Dairy Technol. 62 (2009) 240–248. https://doi.org/10.1111/j.1471-0307.2009.00480.x.

[32] C. Santivarangkna, U. Kulozik, P. Foerst, Inactivation mechanisms of lactic acid starter cultures preserved by drying processes, J. Appl. Microbiol. 105 (2008) 1–13. https://doi.org/10.1111/j.13652672.2008.03744.x.

[33] C. Schwab, R. Vogel, M.G. Gänzle, Influence of oligosaccharides on the viability and membrane properties of *Lactobacillus reuteri* TMW1.106 during freeze-drying, Cryobiology. 55 (2007) 108–114. https://doi.org/10.1016/j.cryobiol.2007.06.004.

[34] I. Siemons, E.M.J. Vaessen, S.E. Oosterbaan van Peski, R.M. Boom, M.A.I. Schutyser, Protective effect of carrier matrices on survival of *Lactobacillus plantarum* WCFS1 during single droplet drying explained by particle morphology development, J. Food Eng. 292 (2021) 110263. https://doi.org/10.1016/j.jfoodeng.2020.110263

[35] Velly H, Bouix M, Passot S, Penicaud C, Beinsteiner H, Ghorbal S, Lieben P, Fonseca F (2015) Cyclopropanation of unsaturated fatty acids and membrane rigidification improve the freeze-drying resistance of *Lactococcus lactis* subsp. *lactis* TOMSC161. Appl Microbiol Biotechnol 99:907–918. https://doi.org/10.1007/s00253-014-6152-2.

[36] W.F. Wolkers, H. Oldenhof, B. Glasmacher, Dehydrating phospholipid vesicles measured in real-time using ATR Fourier transform infrared spectroscopy, Cryobiology. 61 (2010) 108–114. https://doi.org/10.1016/j.cryobiol.2010.06.001.

[37] S. Yeo, H.S. Shin, H.W. Lee, D. Hong, H. Park, W. Holzapfel, E.B. Kim, C.S. Huh, Determination of optimized growth medium and cryoprotective additives to enhance the growth and survival of *Lactobacillus salivarius*, J. Microbiol. Biotechnol. 28 (2018) 718–731. https://doi.org/10.4014/jmb.1801.01059.

[38] G. Zayed, Y.H. Roos, Influence of trehalose and moisture content on survival of *Lactobacillus salivarius* subjected to freeze-drying and storage, Process Biochem. 39 (2004) 1081–1086. https://doi.org/10.1016/S0032-9592(03)00222-X.

[39] Y. Zhang, J. Lin, Q. Zhong, Effects of media, heat adaptation, and outlet temperature on the survival of *Lactobacillus salivarius* NRRL B-30514 after spray drying and subsequent storage, LWT. 74 (2016) 441–447. https://doi.org/10.1016/j.lwt.2016.08.008.

[40] Y.M Zhang, C.O. Rock CO, Membrane lipid homeostasis in bacteria, Nat. Rev. Microbiol. 6 (2008) 222–233. https://doi.org/10.1038/nrmicro1839

Electronic supplementary material

Citation: M. Guerrero Sanchez, S. Passot, S. Ghorbal, S. Campoy, M. Olivares, F. Fonseca, Insights into the mechanisms of *L. salivarius* CECT5713 resistance to freeze-dried storage. Cryobiology. 112 (2023) 104556. (DOI:10.1016/j.cryobiol.2023.104556).

The datasets generated during and/or analysed during the current study are available in the Data INRAE repository: https://doi.org/10.57745/AJO9FD

List of tables

List of figures

Table S1. Production conditions of LAB that have been related to improved resistance to drying, and/or storage showing the main changes observed: modulation of the membrane FA composition, fluidity, lipid organization, and the synthesis of stress and transport-related proteins. The production conditions affording the best resistance to stabilization processes are indicated in bold

Factor	LAB strain	Production condition	Improved resistance to	Change	Reference
Temperature	*L. lactis* subsp. *lactis* MM210	Incubation at 30 °C for 20 min or **heat shock at 42 °C for 25 min** prior to F	FD	Induction or increase in the expression of at least 9 hsps (DnaK, GroEL), (+) cycC19:0	[1]
	L. lactis subsp. *cremoris* MM160 and *L. lactis* subsp. *lactis* MM210	Incubation at 30 °C for 20 min or **cold shock at 10 °C for 2 h** prior to F	FD	Induction in the expression of 8 to 15 csps (DnaK, GroEL), (-) SFA/UFA	[1]
	L. rhamnosus HN001	No heat shock or **heat shock at 50 °C for 30 min** prior to harvest	FBD and FBD storage at 30 °C, 1four weeks	Decrease in the level of enolase and protein HPr, increase in the level of GroEL, DnaK, TBPA, GAP, and TPI	[2]
	L. coryniformis Si3	Fermentation temperature at 26 °C, **34 °C** or **42 °C** after 12 h at 34 °C	FD	NR	[3]
	L. bulgaricus L2	Fermentation temperature at **30 °C**, 35 °C, 37 °C or 39 °C (at controlled pH 5)	FD	(+) cycC19:0/SFA	[4]
	L. salivarius I24	Fermentation temperature uncontrolled or controlled at **37 °C**	FD	NR	[5]
	L. plantarum CFR 2191, *P. acidilactici* CFR 2193, and *L. salivarius* CFR 2158	No cold shock or **cold shock at 8 °C for 2 h** prior to FD	FD	Induction in the expression of csps	[6]
	L. reuteri I5007	Fermentation temperature at 4 °C, 27 °C, 37 °C or **47 °C**	FD	NR	[7]
	L. lactis subsp. *lactis* TOMSC161	Fermentation temperature at 22 °C or **30 °C**	FD and FD storage at 25 °C, 3 months	(+) CFA/UFA	[8]
	L. salivarius NRRL B-3051	No heat shock or **heat shock at 50 °C for 15 min** prior to SD	SD and SD storage at 21 °C, 2 weeks	NR	[9]
pH	*L. delbrueckii* subsp. *bulgaricus*	Controlled **pH** at 6.5 or **uncontrolled**	SD and SD storage at 20 °C, 60 days	Increase in the expression of Hsp70, GroES and GroEL	[10]
	L. coryniformis Si3	Controlled fermentation **pH** at 4.5, **5.5** or 6.5 after 12 h at pH 5.5	FD	(+) SFA/UFA	[3]
	O. oeni SD-2a	Initial fermentation **pH** at 3.2, **3.5**, 4 or 4.8	FD	(+) C19cyc11, (-) C16:0	[11]
	L. bulgaricus L2	Controlled fermentation **pH** at **5**, 5.5, 6 or 6.5 (at 30 °C)	FD	(+) cycC19:0/SFA	[4]
	L. salivarius I24	Uncontrolled fermentation **pH** or controlled at **6.1**	FD	NR	[5]
	O. oeni SD-2a	Initial fermentation **pH** at **3.2**, **3.5**, 4 or 4.8	FD	(+) C19cyc11, (-) C16:0, (+) C14:0, (+) C17cyc9, (+) UFA/SFA	[12]
	L. reuteri I5007	Controlled fermentation **pH** at 4.7, 5.7 or **6.7**	FD	(+) UFA/SFA	[7]
Factor	**LAB strain**	**Condition**	**Improved resistance to**	**Change**	**Reference**

Growth medium	*L. acidophilus*	Medium alone or with **L-ascorbic acid**	FD and FD storage at 21 °C, 20 days	NR	[13]
	L. rhamnosus HN001	No osmotic shock or **osmotic shock (**0.6 M NaCl) prior to harvest	FBD and FBD storage at 30 °C, 1four weeks	Decrease in the level of TPI, PGK, GAP, and protein HPr, increase in the level of GroEL, DnaK, TBPA, and LDH, (+) sugar/protein	[2]
	L. salivarius subsp. *salivarius* UCC 500	**MRS broth with glucose** or trehalose	FD and FD storage at -85 °C, 7 weeks	NR	[14]
	L. delbrueckii subsp. *lactis* FAM-10991	No osmotic stress or **osmotic stress (**1, 1.5, **2.5** or **3.5** % NaCl) during fermentation	FD	NR	[15]
	O. oeni SD-2a	Medium with **glucose**, DL-malate or glucose and DL-malate	FD	(+) C19cyc11, (-) C16:0	[11]
	L. bulgaricus ATCC 11842	No osmotic stress or **osmotic stress (2**, 3.5 or 5 % NaCl for 2 h) during fermentation	FD	Increase in the expression of 6 proteins (elongation factor G, TS, LDH, UMPK, oxidase V), decrease in the expression of 3 proteins (GroEL, IMPDH, glucitol/sorbitol-specific transporter subunit)	[16]
Harvest time	*L. rhamnosus* HN001	Log or **stationary phase**	FBD and FBD storage at 30 °C, 1four weeks	Decrease in the level of GAP and protein HPr, increase in the level of LDH	[2]
	L. rhamnosus GG	**Stationary**, lag or early log **phase**	SD and SD storage at 4, 15 or 37 °C, 8 weeks	NR	[17]
	O. oeni SD-2a	**Early stationary** or mid-exponential phase	FD	(+) C19cyc11, (-) C18:l cis11, (-) C16:0	[11]
	L. lactis subsp. *lactis* TOMSC161	Middle exponential, late exponential, early stationary or **late stationary phase**	FD and FD storage at 25 °C, 3 months	(+) CFA/UFA, (+) SFA, (+) membrane rigidity	[8]
Protective formulation	*L. plantarum* P743	Maltose, trehalose or **sorbitol**	AD	(-) band position of $v_{as}PO_2^-$	[18]
	L. salivarius UCC 500	**Skim milk alone** or with polydextrose	SD and SD storage at 4, 15 or 37 °C, 8 weeks	NR	[17]
	L. salivarius subsp. *salivarius* UCC 500	Sucrose, trehalose, skim milk, sucrose and trehalose, sucrose and skim milk, skim milk and trehalose or **sucrose, trehalose and skim milk**	FD and FD storage at -85 °C, 7 weeks	NR	[14]
	L. rhamnosus GG (ATCC 53103)	**Skim milk alone** or with an oligofructose or a polydextrose	SD and SD storage at 25 or 37 °C, 6 weeks	(+) membrane integrity	[19]
	L. delbrueckii ssp. *bulgaricus* CRL494	**Sodium glutamate** (1.25, 2.5, **5** or 10 %), **sodium aspartate** (1.25, 2.5, **5** or 10 %), maltose (5 or 10 %) or L-proline (2.5 or 5 %)	FD and FD storage at 30 °C, 3 months	(+) membrane fluidity	[20]
	L. reuteri TMW1.106	**Phosphate buffer** alone or **with** skim milk, sucrose, **FOS**, inulin or IMO	FD and FD storage at RT, 14 days	(+) membrane integrity, (+) membrane fluidity	[21]
Factor	**LAB strain**	**Condition**	**Improved resistance to**	**Change**	**Reference**

Protective formulation	*L. delbrueckii* ssp. *bulgaricus* CFL1	Sucrose, maltodextrin, skim milk, skim milk and sucrose or **maltodextrin and sucrose** (2.5 or **5** and **5** %)	AD	Increase in the ability to interact with phospholipids and to stabilize protein structure during drying, strengthening of the glassy matrix	[22]
	L. salivarius I24	**Skim milk** (20, 17.80, 16.55 or **9.85** %), **sucrose** (20, **10.65**, 9.01 or 5.5 %) or glycerol (5 or 3.35 %)	FD	NR	[5]
	L. plantarum CFR 2191, *P. acidilactici* CFR 2193, and *L. salivarius* CFR 2158	Lactose, **maltodextrin** or skim milk	FD storage at 4 °C, 60 days	NR	[6]
	L. salivarius CFR 2158	Skim milk or **maltodextrin**	SD storage at 30 °C, 60 days	NR	[23]
	L. plantarum CFR 2191 and *P. acidilactici* CFR 2193	**Skim milk** or maltodextrin	SD storage at 30 °C, 60 days	NR	[23]
	L. plantarum CWBIB1419 and L. *paracasei* ssp. *paracasei* LMG9192T	**Sorbitol** or monosodium glutamate	FD storage at RT, 120 days	(+) UFA/SFA	[24]
	L. salivarius NRRL B-3051	**Skim milk** alone, with sucrose and trehalose or **with lactose and trehalose**	SD and SD storage at 21 °C, 2 weeks	NR	[9]
	L. salivarius CM-CIDCA 1231B and 1232Y	NaCl, MS, **neutralized MS medium** alone or **with FOS**	FD and FD at 4 °C, 60 days	NR	[25]
	L. salivarius W13	Galactose, lactose, maltose, trehalose, casitone, proteose peptone, yeast extract, skim milk, sucrose, skim milk, and sucrose or **skim milk, sucrose, and sodium glutamate**	FD	NR	[26]

AD: air drying; CFA: cyclic fatty acid; csps: cold shock proteins; FA: fatty acid; FBD: fluid bed drying; FD: freeze-drying; FOS: fructooligosaccharides; GAP: glyceraldehyde-3-phosphate dehydrogenase; HPr: histidine containing proteins; hsps: heat shock proteins; IMO: isomaltooligosaccharides; IMPDH: inosine-5'-monophosphate dehydrogenase; LAB: lactic acid bacteria; LDH: lactate dehydrogenase; MS: malt sprout; NR: no reported; PGK: kinase phosphoglycerate; RT: room temperature; SD: spray-drying; SFA: saturated fatty acid; TBPA: tagatose-6-phosphate aldolase; TPI: triose phosphate isomerase; TS: threonine synthase; UFA: unsaturated fatty acid; UMPK: UMP kinase; $\nu_{as}PO_2^-$: asymmetric PO_2^- stretching band

References Table S1

[1] J.R. Broadbent, C. Lin, Effect of heat shock or cold shock treatment on the resistance of *Lactococcus lactis* to freezing and lyophilization, Cryobiology. 39 (1999) 88–102. https://doi.org/10.1006/cryo.1999.2190.

[2] J. Prasad, P. McJarrow, P. Gopal, Heat and osmotic stress responses of probiotic *Lactobacillus rhamnosus* HN001 (DR20) in relation to viability after drying, Appl. Environ. Microbiol. 69 (2003) 917–925. https://doi.org/10.1128/AEM.69.2.917-925.2003.

[3] Å. Schoug, J. Fischer, H.J. Heipieper, J. Schnürer, S. Håkansson, Impact of fermentation pH and temperature on freeze-drying survival and membrane lipid composition of *Lactobacillus coryniformis* Si3, J. Ind. Microbiol. Biotechnol. 35 (2008) 175–181. https://doi.org/10.1007/s10295-007-0281-x.

[4] C. Li, J.L. Zhao, Y.T. Wang, X. Han, N. Liu, Synthesis of cyclopropane fatty acid and its effect on freeze-drying survival of *Lactobacillus bulgaricus* L2 at different growth conditions, World J. Microbiol. Biotechnol. 25 (2009) 1659–1665. https://doi.org/10.1007/s11274-009-0060-0.

[5] L.C. Ming, R.A. Rahim, H.Y. Wan, A.B. Ariff, Formulation of protective agents for improvement of *Lactobacillus salivarius* I24 survival rate subjected to freeze-drying for production of live cells in powderized form, Food Bioprocess Technol. 2 (2009) 431–436. https://doi.org/10.1007/s11947-009-0184-0.

[6] K.B.P.K. Reddy, S.P. Awasthi, A.N. Madhu, S.G. Prapulla, Role of cryoprotectants on the viability and functional properties of probiotic lactic acid bacteria during freeze-drying, Food Biotechnol. 23 (2009) 243–265. https://doi.org/10.1080/08905430903106811.

[7] X.T. Liu, C.L. Hou, J. Zhang, X.F. Zeng, S.Y. Qiao, Fermentation conditions influence the fatty acid composition of the membranes of *Lactobacillus reuteri* I5007 and its survival following freeze-drying, Lett. Appl. Microbiol. 59 (2014) 398–403. https://doi.org/10.1111/lam.12292.

[8] H. Velly, M. Bouix, S. Passot, C. Penicaud, H. Beinsteiner, S. Ghorbal, P. Lieben, F. Fonseca, Cyclopropanation of unsaturated fatty acids and membrane rigidification improve the freeze-drying resistance of Lactococcus lactis subsp. lactis TOMSC161, Appl Microbiol Biotechnol. 99 (2015) 907–918. https://doi.org/10.1007/s00253-014-6152-2.

[9] Y. Zhang, J. Lin, Q. Zhong, Effects of media, heat adaptation, and outlet temperature on the survival of *Lactobacillus salivarius* NRRL B-30514 after spray drying and subsequent storage, LWT. 74 (2016) 441–447. https://doi.org/10.1016/j.lwt.2016.08.008.

[10] J. Silva, A.S. Carvalho, R. Ferreira, R. Vitorino, F. Amado, P. Domingues, P. Teixeira, P.A. Gibbs, Effect of the pH of growth on the survival of *Lactobacillus delbrueckii* subsp. *bulgaricus* to stress conditions during spray-drying, J. Appl. Microbiol. 98 (2005) 775–782. https://doi.org/10.1111/j.1365-2672.2004.02516.x.

[11] L. Hua, Z. WenYing, W. Hua, L. ZhongChao, W. AiLian, Influence of culture pH on freeze-drying viability of *Oenococcus oeni* and its relationship with fatty acid composition, Food Bioprod. Process. 87 (2009) 56–61. https://doi.org/10.1016/j.fbp.2008.06.001.

[12] W. Zhao, H. Li, H. Wang, Z. Li, A. Wang, The effect of acid stress treatment on viability and membrane fatty acid composition of *Oenococcus oeni* SD-2a, Agric. Sci. China. 8 (2009) 311–316. https://doi.org/10.1016/S1671-2927(08)60214-X.

[13] R. Porubcan, R. Sellars, Stabilized dry cultures of lactic acid-producing bacteria, Patent and Trademark Office. US patent No. 3 897 307 (1975).

[14] G. Zayed, Y.H. Roos, Influence of trehalose and moisture content on survival of *Lactobacillus salivarius* subjected to freeze-drying and storage, Process Biochem. 39 (2004) 1081–1086. https://doi.org/10.1016/S0032-9592(03)00222-X.

[15] S. Koch, G. Oberson, E. Eugster-Meier, L. Meile, C. Lacroix, Osmotic stress induced by salt increases cell yield, autolytic activity, and survival of lyophilization of *Lactobacillus delbrueckii* subsp. *lactis*, Int. J. Food Microbiol. 117 (2007) 36–42. https://doi.org/10.1016/j.ijfoodmicro.2007.01.016.

[16] C. Li, P. Li, J. Sun, G. Huo, L. Liu, Proteomic analysis of the response to NaCl stress of *Lactobacillus bulgaricus*, Biotechnol. Lett. 36 (2014) 2263–2269. https://doi.org/10.1007/s10529-014-1601-7.

[17] B.M. Corcoran, R.P. Ross, G.F. Fitzgerald, C. Stanton, Comparative survival of probiotic lactobacilli spray-dried in the presence of prebiotic substances, J. Appl. Microbiol. 96 (2004) 1024–1039. https://doi.org/10.1111/j.1365-2672.2004.02219.x.

[18] L.J.M. Linders, W.F. Wolkers, F.A. Hoekstra, K. van 't Riet, Effect of added carbohydrates on membrane phase behavior and survival of dried *Lactobacillus plantarum*, Cryobiology. 35 (1997) 31–40. https://doi.org/10.1006/cryo.1997.2021.

[19] E. Ananta, M. Volkert, D. Knorr, Cellular injuries and storage stability of spray-dried *Lactobacillus rhamnosus* GG, Int Dairy J. 15 (2005) 399–409. https://doi.org/10.1016/j.idairyj.2004.08.004.

[20] G. Martos, C. Minahk, G. Font de Valdez, R. Morero, Effects of protective agents on membrane fluidity of freeze-dried *Lactobacillus delbrueckii* ssp. *bulgaricus*, Lett. Appl. Microbiol. 45 (2007) 282–288. https://doi.org/10.1111/j.1472-765X.2007.02188.x.

[21] C. Schwab, R. Vogel, M.G. Gänzle, Influence of oligosaccharides on the viability and membrane properties of *Lactobacillus reuteri* TMW1.106 during freeze-drying, Cryobiology. 55 (2007) 108–114. https://doi.org/10.1016/j.cryobiol.2007.06.004.

[22] H. Oldenhof, W.F. Wolkers, F. Fonseca, S. Passot, M. Marin, Effect of sucrose and maltodextrin on the physical properties and survival of air-dried *Lactobacillus bulgaricus*: an in-situ Fourier Transform Infrared Spectroscopy study, Biotechnol. Progress. 21 (2005) 885–892. https://doi.org/10.1021/bp049559j.

[23] K.B.P.K. Reddy, A.N. Madhu, S.G. Prapulla, Comparative survival and evaluation of functional probiotic properties of spray-dried lactic acid bacteria, Int. J. Dairy Technol. 62 (2009) 240–248. https://doi.org/10.1111/j.1471-0307.2009.00480.x.

[24] I. Coulibaly, R. Dubois-Dauphin, J. Destain, M. Fauconnier, G. Lognay, P. Thonart, The resistance to freeze-drying and to storage was determined as the cellular ability to recover its survival rate and acidification activity, Int. J. Microbiol. 2010 (2010) 1–9. https://doi.org/10.1155/2010/625239.

[25] L. Cejas, N. Romano, A. Moretti, P. Mobili, M. Golowczyc, A. Gómez-Zavaglia, Malt sprout, an underused beer by-product with promising potential for the growth and dehydration of lactobacilli strains, J. Food Sci. Technol. 54 (2017) 4464–4472. https://doi.org/10.1007/s13197-017-2927-7.

[26] S. Yeo, H.S. Shin, H.W. Lee, D. Hong, H. Park, W. Holzapfel, E.B. Kim, C.S. Huh, Determination of optimized growth medium and cryoprotective additives to enhance the growth and survival of *Lactobacillus salivarius*, J. Microbiol. Biotech. 28 (2018) 718–731. https://doi.org/10.4014/jmb.1801.01059.

Table S2. Assignments of the main infrared vibrational bands in the 3016 – 975 cm^{-1} region of the spectra of *L. salivarius* CECT5713 cell populations (S, sensitive and R, resistant) and the main biomolecules associated, according to literature. The changes in the peak height of the second derivative (**Fig. 8a**) after freeze-drying (FD) and storage for four weeks at 37 °C (W4) are also reported

Wavenumber (cm^{-1})		Assignment	Main biomolecule/cellular compound (compartment associated)	Change in the peak height (second derivative) after FD and W4	References
Literature	This work				
2961 2960 2959	2962	νC-H asym of CH_3	Lipids (fatty acyl chain) (membrane)	No change	[27–32]
2930 2929 2925 2918	2924	νC-H asym of CH_2	Lipids (fatty acyl chain) (membrane)	No change	[22,27–30,33]
2882 2875 2874 2873	2873	νC-H sym of CH_3	Lipids (fatty acyl chain) (membrane)	No change	[27–30,34]
2854 2852 2850 2847	2852	νC-H sym of CH_2	Lipids (fatty acyl chain) (membrane)	No change	[22,27–31]
1754 1740 1745 1736	1748	νC=O	Lipids (esters), carbohydrates (peptidoglycan) (membrane, cytoplasm)	No change	[27–29]
1715 1714	1714	νC=O	Nucleic acids (DNA/RNA) (nucleoid, ribosomes)	Increase (FD) R < S Increase (W4) for S	[27,29,31]
1657 1655 1654	1656	Amide I (νC=O) of α-helical structures	Proteins (membrane, cytoplasm)	No change	[22,28,29,31,32,35]
1637 1635	1637	Amide I (νC=O) of β-pleated sheet structures	Proteins (membrane, cytoplasm)	No change	[22,28–32]
1550 1549 1548 1546	1548	Amide II δN-H + νC-N	Proteins (membrane, cytoplasm)	No change	[28–31]
1516-1518 1515	1515	νCC, δCH	Proteins (amino acids, tyrosine) (membrane, cytoplasm)	No change	[31,35]

Wavenumber (cm^{-1})		Assignment	Main biomolecule/cellular compound (compartment associated)	Change in the peak height (second derivative)	References
Literature	**This work**				
1468	1466	C-H deformation of δCH_2 (scissoring)	Proteins, lipids (membrane, cytoplasm)	Increase (FD) R < S Increase (W4) for R	[27,28,31]
1455 1453	1456	C-H deformation of δCH_3 (scissoring)	Proteins, lipids (membrane, cytoplasm)	No change	[27,28,30,32,36]
1415	1417	δC-O-H	Carbohydrates, proteins, nucleic acids (DNA/RNA backbones) (membrane, cytoplasm, nucleoid, ribosomes)	Decrease (FD) S < R Decrease (W4) for R	[30,36]
1415		νC-O sym of COO^-	Lipids (phospholipids) (membrane)		
1402 1401 1400 1400	1400	δCH_3 sym, νCOO^- sym	Proteins (amino acids), carbohydrates (peptidoglycan), lipids (fatty acid) (membrane, cell wall, cytoplasma)	No change	[27,28,30–32,36,37]
1317 1310-1240 1300-1230	1317	Amide III δN-H + νC-N	Proteins (membrane, cytoplasm)	Decrease (FD) S < R Decrease (W4) for R	[28,29,31]
1250 1244	1244	$\nu P{=}O$ asym of PO_2^-	Lipids (phospholipids) (membrane)	No change	[28,36]
1230 1220 1220-1215 1220-1210 1210	1218	$\nu P{=}O$ asym of PO_2^-	Lipid (phospholipids), carbohydrates (teichoic and lipoteichoic acids, peptidoglycan, cell wall fragments), nucleic acids (phosphodiester of DNA/RNA backbones) (membrane, cell wall, nucleoid, ribosomes)	No change	[27–29,31,33,38,39]
1155 1153	1155	νC-O	Proteins, carbohydrates (membrane, cytoplasm)	No change	[27,28]
1122	1122	νC-O	Carbohydrates (membrane, cytoplasm)	No change	[27,28,36]
1120 1118		νC-C sym	Nucleic acids (DNA/RNA backbones) (nucleoid, ribosomes)		
1086 1085 1084 1083	1083	$\nu P{=}O$ sym of PO_2^-	Lipids (phospholipids), carbohydrates (teichoic acids, peptidoglycan, lipopolysaccharides), nucleic acids, proteins (phosphorylated proteins) (membrane, cytoplasm, nucleoid, ribosomes, cell wall)	No change	[27–29,31,32,37]

Wavenumber (cm^{-1})		Assignment	Main biomolecule/cellular compound (compartment associated)	Change in the peak height (second derivative)	References
Literature	This work				
1058	1058	νCO, νC-O-C sym, νP-O-C sym	Carbohydrates (peptidoglycan) (cell wall, membrane, cytoplasm)	Increase (FD) R < S Increase (W4) for R	[27,33,40]
1056					
1055		νPO_2^-, νC-OH, δOCH	Carbohydrates (polysaccharides, oligosaccharides, pectin), nucleic acids (deoxyribose) (cell wall, nucleoid)		[28]
1041	1041	νO–H coupled with δC–O	Carbohydrates (polysaccharides, peptidoglycan) (cell wall)	No change	[27,28]
1040		$\nu P{=}O$ sym of PO_2^-	Nucleic acids (DNA/RNA) (nucleoid, ribosomes)		
1026	1024	CH_2OH, -CH_2OH and νC-O coupled with δC–O of C-OH	Carbohydrates (glucose, fructose, glycogen) (cytoplasm)	Increase (FD, W4) R < S	[27,28]
1024-1025					
996	995	νC-O ribose, νC-C	Nucleic acids (ribose skelet RNA) (ribosomes)	No change	[27,28]
993					

ν: stretching, δ: bending, sym.: symmetric, asym.: asymmetric

References Table S2

[27] F. Quilès, F. Humbert, A. Delille, Analysis of changes in attenuated total reflection FTIR fingerprints of *Pseudomonas fluorescens* from planktonic state to nascent biofilm state, Spectrochim Acta A Mol. Biomol. Spectrosc. 75 (2010) 610–616. https://doi.org/10.1016/j.saa.2009.11.026.

[28] Z. Movasaghi, S. Rehman, D.I. ur Rehman, Fourier Transform Infrared (FTIR) spectroscopy of biological tissues, Appl Spectrosc Rev. 43 (2008) 134–179. https://doi.org/10.1080/05704920701829043.

[29] A. Girardeau, S. Passot, J. Meneghel, S. Cenard, P. Lieben, I.C. Trelea, F. Fonseca, Insights into lactic acid bacteria cryoresistance using FTIR microspectroscopy, Anal Bioanal Chem. 414 (2022) 1425–1443. https://doi.org/10.1007/s00216-021-03774-x.

[30] J.M. LeGal, M. Manfait, T. Theophanides, Applications of FTIR spectroscopy in structural studies of cells and bacteria, J Mol Struct. 242 (1991) 397–407. https://doi.org/10.1016/0022-2860(91)87150-G.

[31] D. Naumann, Infrared spectroscopy in microbiology, in: R.A. Meyers (Ed.), Encyclopedia of Analytical Chemistry, John Wiley & Sons Ltd, Chichester, 2000: pp. 102–131.

[32] M.I. Santos, E. Gerbino, E. Tymczyszyn, A. Gomez-Zavaglia, Applications of infrared and Raman spectroscopies to probiotic investigation, Foods. 4 (2015) 283–305. https://doi.org/10.3390/foods4030283.

[33] M.M. Hlaing, B.R. Wood, D. McNaughton, D. Ying, G. Dumsday, M.A. Augustin, Effect of drying methods on protein and DNA conformation changes in *Lactobacillus rhamnosus* GG cells by Fourier Transform Infrared Spectroscopy, J. Agric. Food Chem. 65 (2017) 1724–1731. https://doi.org/10.1021/acs.jafc.6b05508.

[34] K. Kochan, H. Peng, E.S.H. Gwee, E. Izgorodina, V. Haritos, B.R. Wood, Raman spectroscopy as a tool for tracking cyclopropane fatty acids in genetically engineered *Saccharomyces cerevisiae*, Analyst. 144 (2019) 901–912. https://doi.org/10.1039/C8AN01477A.

[35] A. Barth, Infrared spectroscopy of proteins, Biochim Biophys Acta. 1767 (2007) 1073–1101. https://doi.org/10.1016/j.bbabio.2007.06.004.

[36] C. Yu, J. Irudayaraj, Spectroscopic characterization of microorganisms by Fourier Transform Infrared microspectroscopy, Biopolymers. 77 (2005) 368–377. https://doi.org/10.1002/bip.20247.

[37] K.B. Beć, J. Grabska, C.W. Huck, Biomolecular and bioanalytical applications of infrared spectroscopy – a review, Analytica Chimica Acta. 1133 (2020) 150–177. https://doi.org/10.1016/j.aca.2020.04.015.

[38] J. Meneghel, S. Passot, F. Jamme, S. Lefrançois, P. Lieben, P. Dumas, F. Fonseca, FTIR micro-spectroscopy using synchrotron-based and thermal source-based radiation for probing live bacteria, Anal Bioanal Chem. 412 (2020) 7049–7061. https://doi.org/10.1007/s00216-020-02835-x.

[39] W. Jiang, A. Saxena, B. Song, B.B. Ward, T.J. Beveridge, S.C.B. Myneni, Elucidation of functional groups on gram-positive and gram-negative bacterial surfaces using infrared spectroscopy, Langmuir. 20 (2004) 11433–11442. https://doi.org/10.1021/la049043.

[40] A.M. Melin, A. Allery, A. Perromat, C. Bébéar, G. Déléris, B. de Barbeyrac, Fourier transform infrared spectroscopy as a new tool for characterization of mollicutes, J. Microbiol. Methods. 56 (2004) 73–82. https://doi.org/10.1016/j.mimet.2003.09.020.

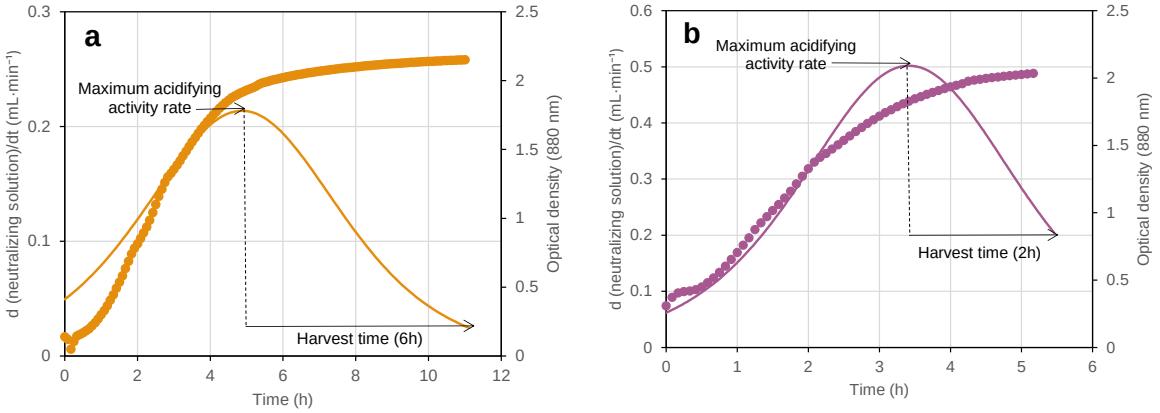

Figure S1. Cell growth (controlled by optical density measurement at 880 nm (●)) and acidifying activity rate (from the first derivative of the neutralizing solution consumption (—)) of two *L. salivarius* CECT5713 cell populations ((**a**) sensitive and (**b**) resistant). Cells were harvested at two varying times (t = 6 and 2 h) after reaching the maximum acidifying activity rate

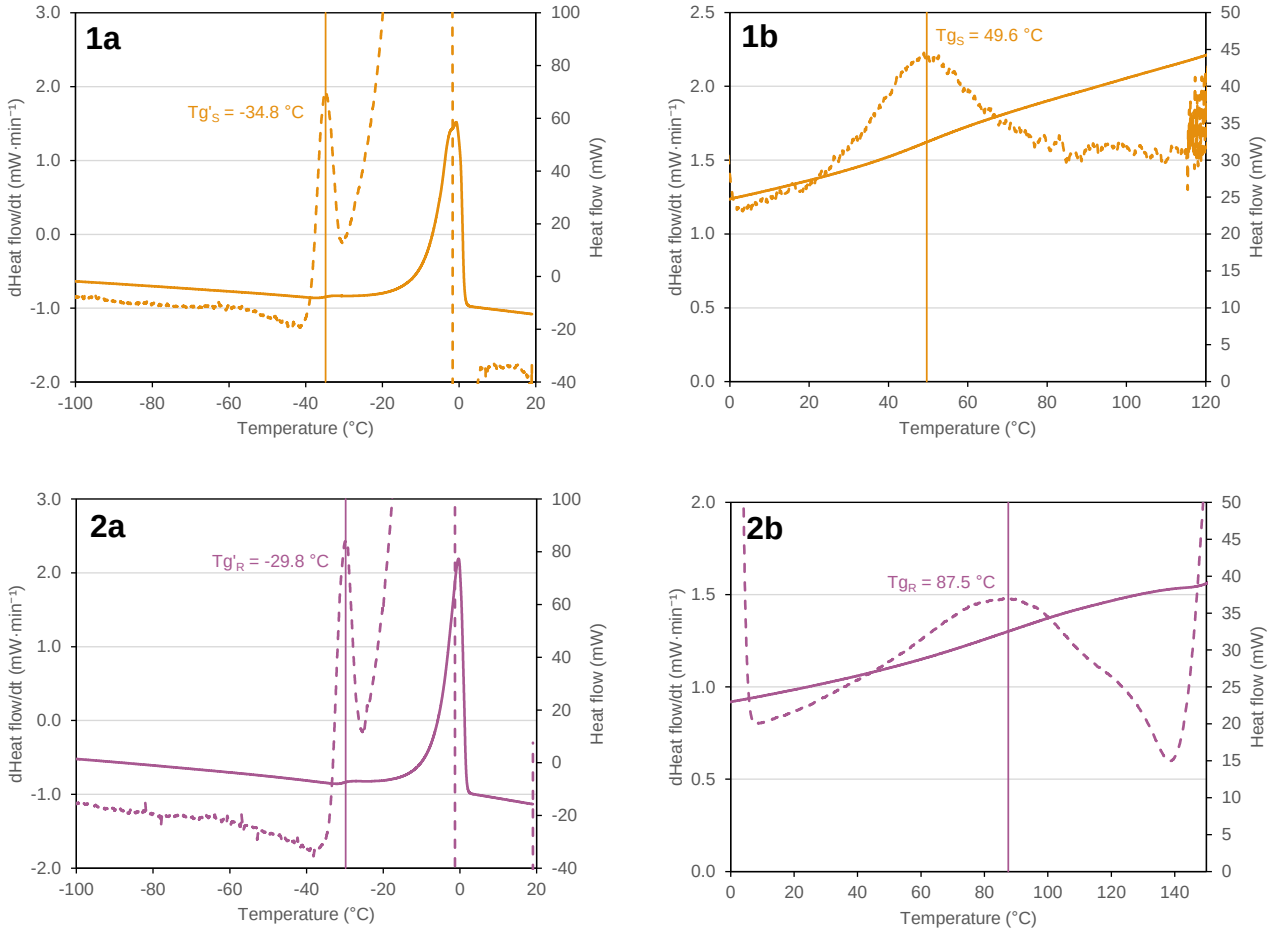

Figure S2. Measure of the glass transition temperature of (**a**) bacterial concentrates and (**b**) freeze-dried powders of two *L. salivarius* CECT5713 cell populations ((**1**) sensitive and (**2**) resistant). The curves correspond to the heat flow (—) as a function of temperature and its smoothed first derivative (---). The vertical line indicates the glass transition temperature value (Tg' and Tg) calculated from the maximum of the first derivative

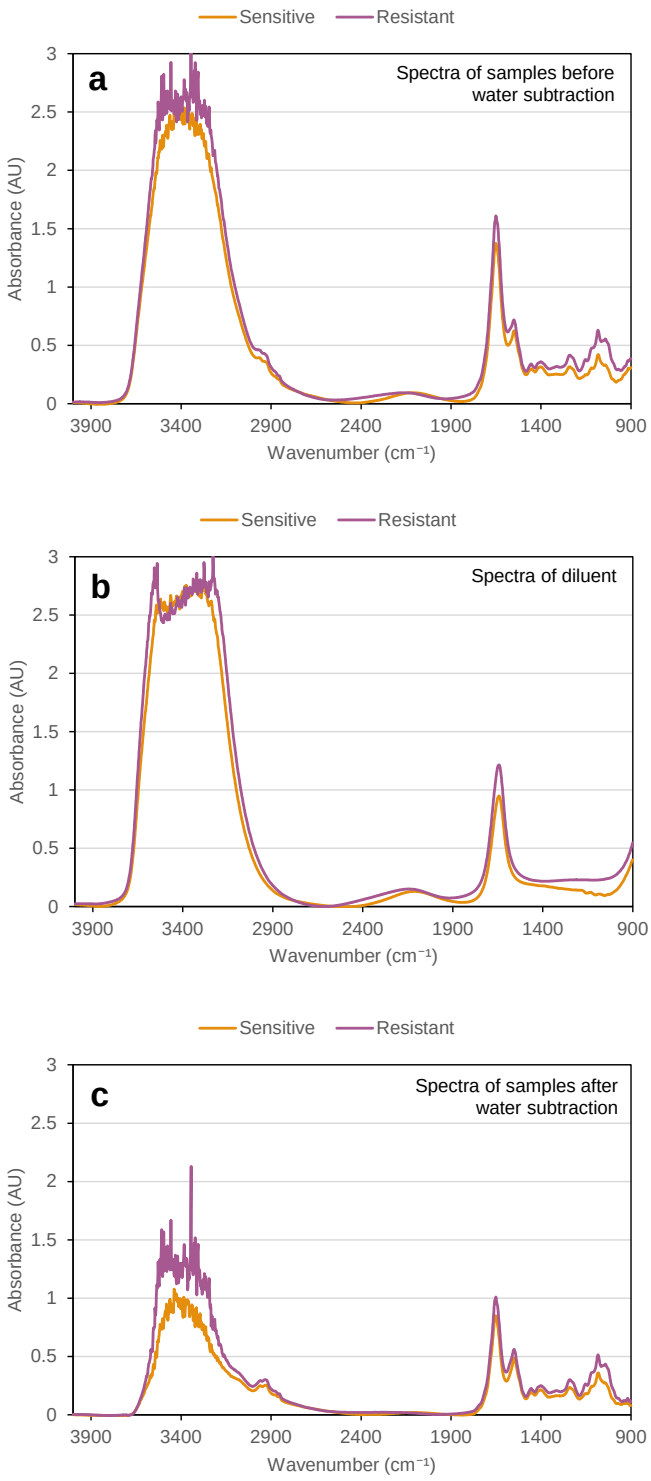

Figure S3. Illustration of the water subtraction procedure applied to the spectra of two *L. salivarius* CECT5713 cell populations (sensitive and resistant) showing (**a**) spectra of samples recorded in an aqueous environment, (**b**) spectra of diluent, and (**c**) the result of the subtraction between the spectra of samples and the spectra of diluent

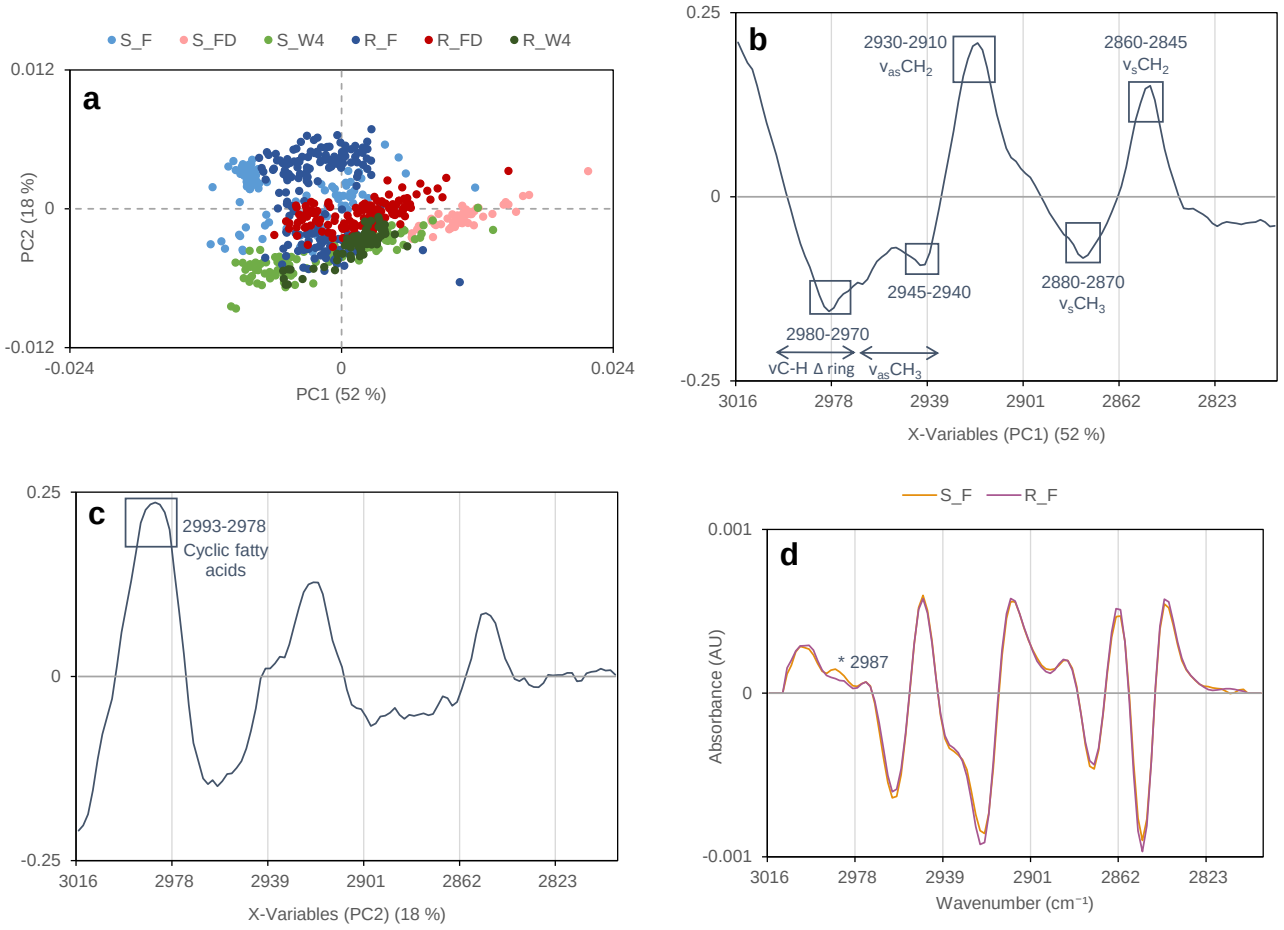

Figure S4. Principal component analysis (PCA) of FTIR normalized and corrected spectra of frozen (F), freeze-dried (FD), and stored for four weeks at 37 °C (W4) of two *L. salivarius* CECT5713 cell populations (S, sensitive and R, resistant) in an aqueous environment, in the 3016 – 2800 cm^{-1} region. (**a**) PC1 versus PC2 score plots explain 52 and 18 % of the variance, respectively. (**b**) Loading plot of the PC1. (**c**) Loading plot of the PC2: positive peaks slightly characterized the frozen cells, whereas negative peaks slightly characterized the freeze-dried and stored cells. (**d**) Mean second derivative of the normalized spectra of the frozen sensitive and resistant cells, showing the peak that has been associated with cyclic fatty acids (2987 cm^{-1})